



Decoupling salinity and carbonate chemistry: Low calcium ion concentration rather than salinity limits calcification in Baltic Sea mussels

5 Trystan Sanders^{1*}, Jörn Thomsen¹, Jens Daniel Müller², Gregor Rehder³, Frank Melzner¹

¹Marine Ecology, Helmholtz Centre for Ocean Research (GEOMAR), Kiel, Germany

²Environmental Physics, Institute of Biogeochemistry and Pollutant Dynamics, ETH Zurich, Zurich, Switzerland.

³Department of Marine Chemistry, Leibniz Institute for Baltic Sea Research, Warnemünde, Germany

10

Correspondence to: Trystan Sanders, (trystanbrett@gmail.com)

Abstract

15 The Baltic Sea has a salinity gradient decreasing from fully marine (> 25) in the West to below 7 in the Central Baltic Proper. Reef forming mytilid mussels exhibit decreasing growth when salinity < 11, however the mechanisms underlying reduced calcification rates in dilute seawater are not fully understood. In fact, both [HCO₃⁻] and [Ca²⁺] also decrease with salinity, challenging calcifying organisms through CaCO₃ undersaturation ($\Omega \leq 1$) and unfavourable ratios of calcification substrate (Ca²⁺ and HCO₃⁻) to inhibitor (H⁺). In this study we assessed the impact of isolated individual factors (salinity, [Ca²⁺], [HCO₃⁻] and pH) on calcification and growth of mytilid mussel populations along the Baltic salinity gradient. Laboratory experiments rearing juvenile Baltic *Mytilus* at a range of salinities (6, 11 and 16), HCO₃⁻ concentrations (300-2100 $\mu\text{mol kg}^{-1}$) and Ca²⁺ concentrations (0.5-4 mmol kg⁻¹) were coupled with field monitoring in three Baltic mussel reefs. Results reveal that as individual factors, low [HCO₃⁻], pH and salinity cannot explain low calcification rates in the Baltic Sea. Calcification rates are impeded when $\Omega_{\text{aragonite}} \leq 1$ or the substrate inhibitor ratio ≤ 0.7 , primarily due to [Ca²⁺] limitation which corresponds to a salinity of ca. 11. Increased food availability may be able to mask these negative impacts, but not when seawater conditions are permanently adverse, as observed in two Baltic reefs at salinities < 11. Future climatic models predict rapid desalination of the southwest and Central Baltic and potentially a reduction in [Ca²⁺] which may lead to a westward distribution shift of marine calcifiers. It is therefore vital to understand the mechanisms by which the ionic composition of seawater impacts bivalve calcification for better predicting the future of benthic Baltic ecosystems.

30

1. Introduction

The Baltic Sea is a semi-enclosed brackish water body with a decreasing salinity (S) gradient from > 25 in the Kattegat to salinities < 3 in the Gulf of Bothnia and the Gulf of Finland (Meier, 2006; Neumann, 2010; Fig. 1). Seawater total alkalinity (A_T) decreases linearly along this salinity gradient from ~ 2300 $\mu\text{mol kg}^{-1}$ in the North Sea as the marine endmember to ~ 1600 $\mu\text{mol kg}^{-1}$ at a salinity of 6 in the Baltic Proper (Müller, et al., 2016). In seawater that is in equilibrium with current atmospheric pCO₂, the dissolved bases HCO₃⁻ and CO₃²⁻ comprise ca. 96% of A_T. Since these two carbon species make-up ca. 99 % of all total dissolved inorganic carbon (C_T), both A_T and C_T are tightly coupled (Zeebe and Wolf-Gladrow, 2007). As well as C_T, seawater [Ca²⁺] also decreases linearly with salinity from the North Sea to the Baltic Proper (Kremling and Wilhelm, 1997) which has implications for marine calcifying organisms that utilise these 2 substrates (Ca²⁺ and dissolved inorganic carbon) for calcification. Although CaCO₃ is ultimately formed from Ca²⁺ and CO₃²⁻, evidence suggests that rather than CO₃²⁻, dissolved HCO₃⁻ is the primary source of inorganic carbon for calcification in marine organisms (Bach, 2015). This is because HCO₃⁻ is ca. 10-fold more abundant in seawater than CO₃²⁻ (in seawater at equilibrium with current atmospheric pCO₂) and HCO₃⁻ transporters have been localised in the calcifying tissues of marine organisms (Roleda, et al., 2012; Zoccola, et al., 2015; Fassbender, et al., 2016; Hu, et al., 2018).

Despite reduced salinity and availability of calcification substrate (Ca²⁺ and HCO₃⁻) along the Baltic Sea salinity gradient, calcifying mytilid mussels in the genus *Mytilus* dominate the Baltic benthos forming extensive biogenic reefs, biodiversity hotspots and contributing significantly to nutrient recycling and aquaculture (Norling and Kautsky, 2008; Kotta, et al., 2020). Baltic *Mytilus* play a central role in the regions' ecosystems, despite drastically reduced calcification rates below a salinity of 11, resulting in extremely slow growing mussels with thin shells and small maximum body sizes (Kautsky, et al., 1990; Vuorinen, et al., 2002; Riisgård, et al., 2014; Sanders, et al., 2018). Such slow calcification and growth rates in Baltic *Mytilus* have been attributed to unfavourable protein metabolism from osmotic stress and high energetic costs of CaCO₃ biomineralisation (Tedengren and Kautsky, 1986; Maar, et al., 2015; Sanders, et al. 2018; Thomsen, et al., 2018). Until now, the effects of salinity as a sole factor on growth has not been investigated separately from calcification substrate availability.

50

55



The stability of CaCO_3 structures in seawater is related to the saturation state (Ω) of the CaCO_3 polymorph in question (predominantly aragonite or calcite), which is defined as:

60

$$\Omega = \frac{[\text{Ca}^{2+}][\text{CO}_3^{2-}]}{K_{sp}} \quad (1)$$

with K_{sp} being the temperature, pressure and salinity-dependent solubility product of the CaCO_3 polymorph under consideration. CaCO_3 dissolution becomes more thermodynamically favourable when $\Omega < 1$ (undersaturation), having major implications for marine organisms which biomineralize external CaCO_3 structures (Waldbusser, et al., 2014; Ries, et al., 2016). Extended periods of undersaturation of the CaCO_3 polymorph aragonite ($\Omega_{\text{aragonite}} \leq 1$), are commonplace in the Baltic Sea, theoretically imposing constraints on calcifying organisms that precipitate aragonite CaCO_3 crystals, as mytilid mussels do for production of inner shell nacre (Tyrrell, et al., 2008; Melzner, et al., 2011). Severe desalination and warming is predicted over the next 50 – 100 years, due to changes in weather patterns and precipitation, yet our ability to predict future carbonate chemistry changes remains somewhat limited in the Baltic Sea due to potential antagonistic effects of desalination and continental weathering (Gräwe, et al., 2013; Müller, et al., 2016).

Despite $\Omega_{\text{aragonite}}$ being a good predictor for biological calcification especially at fully marine conditions, there is little evidence supporting its mechanistic role in biocalcification. Even with a rudimentary understanding of calcification mechanisms in molluscs, we know that increased $[\text{H}^+]$ inhibits extracellular calcification by increasing the proton gradient between the calcifying fluid and seawater (Ramesh, et al., 2017; Sevilgen, et al., 2019). Additionally, since HCO_3^- is likely the primary carbon species used in calcification (see previous paragraph) and its availability stimulates CaCO_3 biomineralisation, a more accurate and mechanistically relevant predictor for biocalcification is the substrate (HCO_3^-) inhibitor (H^+) ratio or SIR (Jokiel, et al., 2013; Bach, 2015; Thomsen, et al., 2015; Cyronak, et al., 2016.). Concentrations of Ca^{2+} are high and generally constant ($\sim 10 \text{ mmol kg}^{-1}$) at oceanic salinities and are resultingly excluded in calculating SIR, expressed in Eq. (2). At salinities < 8 however, limitation of seawater Ca^{2+} has been shown to reduce calcification in larval Baltic *Mytilus* (Thomsen, et al., 2018), therefore adopting an extended SIR (ESIR) to include $[\text{Ca}^{2+}]$, may provide an even more accurate predictor of calcification under low saline conditions:

85

$$\text{SIR} = [\text{HCO}_3^-] / [\text{H}^+] \quad (2)$$

90

$$\text{ESIR} = \frac{[\text{Ca}^{2+}][\text{HCO}_3^-]}{[\text{H}^+]} \quad (3)$$

Bivalve calcification in the Baltic Sea drops significantly when $\text{ESIR} \leq 0.7$ (Thomsen, et al., 2018). Application of the ESIR is particularly important in coastal and estuarine zones such as the Baltic, where freshwater input, photosynthetic activity and wind-driven upwelling can delineate carbonate system parameters (pH and pCO_2) from salinity and weaken the predictive power of SIR for calcification (Melzner, et al., 2013; for more detail see Fassbender, et al., 2016).

Environmental variability is high on both spatial and temporal scales in the Baltic Sea with variations in carbonate chemistry and salinity resulting from occasional inflow events of highly saline North Sea water, wind driven upwelling of hypoxic and hypercapnic deep water, lateral transport of water masses and pronounced regional salinity gradients (Thomas and Schneider, 1999; Melzner, et al., 2013; Saderne, et al., 2013; Mohrholz, et al., 2015). Eutrophication promotes phytoplankton blooms, which vary in intensity between different Baltic basins providing vital sources of energy for secondary consumers (HELCOM, 2014, Gustafsson, et al., 2019; Hjerne, et al., 2019). High phytoplankton food availability correlates with improved reproductive condition in mussels and has been shown to counteract the negative effects of sub-optimal carbonate chemistry on calcification in Baltic *Mytilus* in Kiel Fjord (Wołowicz, et al., 2006; Melzner, et al., 2011; Thomsen, et al., 2013). Additionally, macrophyte habitats can mitigate the negative effects of seawater acidification on calcifiers by increasing pH in adjacent seawater (Wahl, et al., 2017). The complex interactions between multiple environmental factors impacting calcification makes predicting present and future calcification rates of the ecologically important reef forming Baltic mussel difficult. Further elucidation on how salinity and carbonate chemistry control mollusc calcification and how these environmental factors fluctuate in Central and southwest Baltic mussel reefs is vital to predict the impacts of marine climate change on benthic Baltic ecosystems.

The overarching aim of this study was to investigate how calcification in Baltic *Mytilus* is controlled by natural variation in carbonate chemistry along the southwest Baltic Sea salinity gradient. Laboratory experiments decoupling salinity from calcification substrates (HCO_3^- and Ca^{2+}) and pH were employed to investigate how



120 these parameters individually control calcification rates. This was combined with a multi-year monitoring programme of salinity, carbonate chemistry, temperature, food availability and calcification rates in three mussel reefs along the German Baltic salinity gradient to shed light on how *in situ* calcification rates are controlled by salinity, carbonate chemistry and food availability.

2. Material and Methods

2.1 Animal collection and maintenance conditions

125 A genetic hybrid zone and gradient in allele frequencies exists in the southwest Baltic Sea from > 90 % Baltic *Mytilus edulis* dominated hybrids at higher salinities (> 16) to > 90 % Baltic *Mytilus trossulus* hybrids at low salinities (< 8), with a genetic transition zone occurring at salinities of 10-12 (Stuckas et al. 2017). Two cohorts of freshly settled Baltic *Mytilus* from the genetic transition zone (mean shell length, SL = 0.6 mm - cohort 1, and 3.0 mm - cohort 2) were collected from wooden pillars in Ahrenshoop, Germany (54° 23' 13" N, 12° 25' 37" E., mean salinity = 10.8, temperature = 19.3 °C, depth < 1 m) in July 2014 and 2016 (Fig. 1). Animals were transported within 6 h in chilled, aerated cool boxes to GEOMAR, Kiel, stored in 20 L plastic aquaria (16 °C) for three weeks prior to experiments and fed twice daily with live *Rhodomonas salina* to achieve an aquarium concentration of > 10 000 cells ml⁻¹. Water was exchanged every three days and the correct salinity was obtained by mixing 0.22 µm filtered seawater (FSW) from Kiel Fjord (salinity ~ 16) with distilled water and adjusting A_T to natural values via addition of 1M NaHCO₃ solution.

135

2.2 [HCO₃⁻] and [Ca²⁺] manipulation experiments

140 Two laboratory experiments were conducted to investigate the effects of calcification substrate availability (HCO₃⁻ and Ca²⁺) on calcification. The first experiment exposed Baltic *Mytilus* juveniles (cohort 1, mean SL = 0.6 mm) to three salinities (16, 11 and 6, spanning the salinity gradient of the southwest Baltic Sea) and six bicarbonate ion concentrations (300, 600, 900, 1500, and 2100 µmol kg⁻¹), reflecting A_T of full strength seawater down to salinities < 3 in the northern Baltic Sea (Müller, et al., 2016). The experiment lasted 70 days and was conducted in 2 L plastic aquaria each containing ~ 1600 animals with four replicate aquaria per treatment (15 treatments, 60 aquaria in total). Seawater carbonate chemistry and salinity manipulation was done by diluting FSW from Kiel Fjord to experimental salinities (16, 11 and 6) with distilled water in 800 L containers. C_T and pH_{NBS} were determined weekly in stock FSW and experimental FSW (see section: 2.3). To achieve experimental [HCO₃⁻] values, 1M NaHCO₃ or 1M HCl was added to increase or decrease [HCO₃⁻], respectively (summaries of all water parameters are given in Table 1). Water was prepared individually for each treatment aquarium 24 h before water changes and aerated with ambient pressurized air at atmospheric pCO₂ equilibrium.

150 A second experiment was conducted to investigate the impact of [Ca²⁺] on calcification rates. This experiment utilised a similar experimental design to the first experiment, exposing juvenile Baltic *Mytilus* (cohort 2, mean SL = 3.0 mm) to the same three salinities (16, 11 and 6) and five different [Ca²⁺] values (0.5, 1, 2, 3, 4 mmol kg⁻¹) covering the natural range of [Ca²⁺] in the southwest and Central Baltic (Thomsen, et al., 2018). Experimental seawater was manipulated through the preparation of Ca²⁺ free artificial seawater (CFASW) in three stock solutions (salinity 6, 11 and 16) by adding NaCl, NaSO₄, KCl, NaHCO₃, KBr, H₃BO₃, MgCl₂ and SrCl₂ to deionised water (Table S1; details in Kester, 1967). At each stock salinity, [Ca²⁺] was adjusted through the addition of a 1 M CaCl₂ stock solution to achieve experimental concentrations. Weekly water samples were taken for measuring C_T and [Ca²⁺] in stock CFASW and experimental aquaria. [Ca²⁺] was measured using a flame photometer (EFOX 5053, Eppendorf) calibrated with urine standards (Biorapid; see Table 2 for water parameters summary). Aquarium volumes in the Ca²⁺ experiment could not be as high as in the HCO₃⁻ experiment due to an inability to produce large volumes of CFASW. Subsequently, the Ca²⁺ experiment was conducted in smaller 50 ml plastic aquaria with two animals per tank and four replicates (15 treatments, 60 aquaria in total) and lasted 37 days. Fewer animals were used per aquarium to minimise the impact of biomineralisation on seawater carbonate chemistry in these smaller water volumes.

165

170 While it may be argued that this disparity in aquarium volumes and animal numbers makes comparisons between both experiments more difficult, measures were taken to ensure comparable conditions between both experiments (Table S2). Live microalgal food (*R. salina*) was added once per day in the Ca²⁺ experiment and twice daily in the HCO₃⁻ experiment (this later increased to thrice daily as animals grew) to achieve a final cell concentration in each aquarium of > 10 000 cells ml⁻¹ and a comparable level of daily food ration between both experiments (no. cells mg⁻¹ of dry mass, see Table S2 for further details). Cell concentrations in microalgae cultures were monitored daily using a Multisizer 3 Coulter Counter (Beckman, Germany). In both experiments, aquaria were held in 16 °C water baths and the mean total body mass per litre in experimental aquaria (mean experimental value) was comparable between both experiments (Table S2) to limit the impacts of biomass on aquaria carbonate chemistry. Water changes were conducted two to three times weekly to minimise deviation in experimental carbonate

175



chemistry parameters. At the end of both experiments, calcification rates were calculated (section 2.4 calcification rates) in $\mu\text{g CaCO}_3 \text{ d}^{-1}$.

2.3 Carbonate chemistry

180 For laboratory carbonate chemistry, pH_{NBS} was measured three times weekly using a WTW pH 3110 probe at 25 °C calibrated with two standard precision NBS buffers (Radiometer analytical) at pH 7.0 and 10.0. Experimental temperature and salinity were monitored daily using a WTW Cond 315i probe. C_T was analysed using an AIRICA CO_2 analyser (Marianda, Kiel, Germany) calibrated by measuring certified reference material (Dickson, et al., 2003). Experimental seawater carbonate system parameters (A_T , $[\text{H}^+]$, $[\text{HCO}_3^-]$, $[\text{CO}_3^{2-}]$, and $\Omega_{\text{aragonite}}$) were calculated with C_T and pH_{NBS} as inputs using the CO2Sys_v2.1 program (KHSO₄ constants from Dickson, et al., 1990, K1 and K2 dissociation constants from Millero, 2010). Values for $\Omega_{\text{aragonite}}$ in the calcium experiment were calculated according to Eq. (1) from measured $[\text{Ca}^{2+}]$ in each technical replicate, as well as calculated $[\text{CO}_3^{2-}]$ and K_{sp} . The SIR and ESIR were calculated according to Eq. (2) and Eq. (3).

2.4 Calcification rates

190 Calcification rates were determined by calculating the change in individual CaCO_3 mass over time. Individual mass of CaCO_3 (mg) at the end of the experiment (t_1) was determined by removing body tissue from individuals using forceps under a stereomicroscope and placing empty shells individually into pre-weighed and pre-dried aluminium foil cups which were then placed in a muffle furnace and ashed at 450 °C for 4 h to remove all organic content. The remaining inorganic ash mass of the shell was used as a proxy for CaCO_3 mass. Individual CaCO_3 mass at the beginning of each experiment (t_0) was calculated from the mean initial SL per replicate tank and using the SL- CaCO_3 mass relationship for juvenile mussels from the same population (Sanders, et al., 2018, Fig. S1). The difference between the mean individual CaCO_3 mass per replicate at t_0 and t_1 is the total calcification per individual. CaCO_3 mass was converted to μg and total calcification was divided by the experimental duration (days) to arrive at the calcification rate in $\mu\text{g CaCO}_3 \text{ d}^{-1}$.

2.5 Field monitoring

205 Three monitoring sites were selected along the German Baltic Sea coast, spanning the geographic range of the steepest salinity and Baltic *Mytilus* genetic gradient (Fig. 1). These sites were: Kiel (54° 19' 49" N, 10° 8' 60" E), Ahrenshoop (54° 23' 7" N, 12° 25' 24" E) and Usedom (54° 3' 21" N, 14° 0' 40" E). Mini CTD (conductivity, temperature, depth) loggers (Star-Oddi, Iceland) logging data every 3 h, were deployed on wooden pillars at each site between July and Sept. 2015 (0.5-1.5 m depth) and replaced every 2-3 months until Jan. 2018. Field $[\text{Ca}^{2+}]$ was calculated from salinity values using $[\text{Ca}^{2+}]$ -chlorinity relationships from Kremling and Wilhelm, 1997 and a chlorinity-salinity relationship from Millero, 1984. Reference measurements from field water samples concurred with these calculations from the literature (Fig. S2). Additionally, every 2-3 months, two 500 ml water samples were taken from Ahrenshoop and Usedom (1 m depth) and immediately poisoned with saturated HgCl_2 solution (0.5 % final concentration) for pH_{total} , A_T and C_T measurements at the Leibniz Institute for Baltic Sea Research, Warnemünde. Kiel carbonate chemistry data was taken from published monitoring data for Jan.-Dec. 2015 (Hiebenthal, et al., 2017). Water pH_{total} was measured spectrophotometrically at 25 °C with non-purified m-cresol purple as indicator dye (pH calculated according to Müller and Rehder, 2018, dye pH-perturbation corrected after Hammer, et al., 2014). C_T was determined with a SOMMA system (Single Operator Multi-Parameter Metabolic Analyzer) operated at 15°C and A_T was determined by open-cell titration at 20 °C (Dickson, et al., 2007). Field carbonate chemistry parameters were calculated using C_T and pH_{total} as inputs with the same constants described previously (section 2.3).

2.7 Field mussel growth

220 In March 2016, mussel settlement structures ($n =$ three per site) were placed at each site to monitor the growth of the spring cohort of settled juveniles over the course of 15 months. The structures were made from a 35 cm long cylinder of grey PVC pipe with a diameter of 10 cm. Twenty 2 cm diameter holes were drilled into the sides and a 0.2 mm gridded nylon net (standard seed sock for mussel aquaculture) was placed diagonally across the inside to increase surface area allowing for maximum settlement (Fig. S3). These settlement structures were cable tied to wooden pillars at each site at ca. 0.5-1 m depth and samples of 50 juvenile mussels were taken for shell length measurements from each site every 2-3 months. Individual shell mass (SM, $\mu\text{g CaCO}_3$) was calculated using SL- CaCO_3 relationships for each population from Sanders, et al., 2018 (Fig. S1). To allow direct comparison between sites, individual calcification rates ($\mu\text{g CaCO}_3 \text{ d}^{-1}$) are expressed as the linear slopes of CaCO_3 mass over time (days) over the first 3 sampling time points before growth rates deviate from linear.

2.8 Food availability

235 Chlorophyll-*a* (chl-*a*) concentrations ($\mu\text{g L}^{-1}$) were used as a proxy for phytoplankton food availability in Baltic Sea surface waters (Wasmund, et al., 2011). Values for chl-*a* concentrations at the three monitoring sites were



240 obtained from field monitoring data supplied by the Landesamt für Landwirtschaft, Umwelt und ländliche Räume (LLUR) sampled from Mönkeberg (54° 21' 7" N, 10° 10' 36" E), 2.5 km from the field monitoring site in Kiel Fjord. Chl-*a* monitoring data for Ahrenshoop and Usedom were supplied by the Landesamt für Umwelt, Naturschutz und Geologie (LUNG) sampled from near Fischland (54° 20' 43" N, 12° 26' 55" E), 1 km from the sampling site in Ahrenshoop and Zinnowitz (54° 4' 57" N, 13° 54' 57" E), 4 km from the monitoring site in Usedom.

2.9 Data analysis

245 All data analysis was conducted using R Software version 3.6.3 (R Core Team, 2020) with all packages used listed in Table S4. Data distributions were tested for normality (Shapiro-Wilk test) and homogeneity of variances (Levene's test) before running parametric tests. In the bicarbonate experiment, a negative exponential decay model was fit to the relationship between $[\text{HCO}_3^-]$ and calcification rate using a nonlinear least squares method for parameter optimisation. The Akaike Information Criterion (AIC) was used to designate the most parsimonious model (Table S5). Linear regression models were fit to calcification rates with $[\text{Ca}^{2+}]$ as a co-variate and salinity as a factor in the calcium experiment. Negative exponential decay models were fit to explain the relationship between ESIR and $\Omega_{\text{aragonite}}$ on laboratory calcification rates with model parameters (C_{max} and K) compared (showing 95 % confidence intervals) between ESIR and $\Omega_{\text{aragonite}}$ as predictors of calcification. The residual sum of squares (RSS) was used as a measure of model fit. The impacts of salinity were analysed statistically by comparing the C_{max} parameter (± 95 % confidence interval) of the non-linear model in the bicarbonate experiment and ANCOVA in the calcium experiment. Field calcification rates (monthly means) and environmental parameters (salinity, pH, chl-*a*, $[\text{Ca}^{2+}]$, $[\text{HCO}_3^-]$, $\Omega_{\text{aragonite}}$, and ESIR) were analysed using parametric tests (ANCOVA) with time as a co-variate for field calcification rates and site as a fixed factor. Pairwise comparisons were conducted on significant factors by way of a Tukey test. Field temperatures for the given monitoring period (2015-2017) were analysed non-parametrically using a Kruskal-Wallis test. Finally, field calcification rates were calculated as the values for the linear slopes of cumulative calcification over time for the first three sampling periods. Log transformed mean calcification rates for each site were plotted against mean values for individual field environmental parameters.

3. Results

3.1 Calcification

265 Calcification rates in the bicarbonate experiment exhibited a significant negative exponential decay relationship with decreasing $[\text{HCO}_3^-]$ (Table S7), with calcification rates decreasing most abruptly below ca. 1000 $\mu\text{mol kg}^{-1}$ (Fig. 2a) at salinities of 11 and 16. Maximum calcification rates (C_{max}) at salinity 6 were only ~ 13 % of those at 11 and 16 and not statistically different between 11 and 16 (Fig. 2c). The subsequent experiment which decoupled $[\text{Ca}^{2+}]$ from salinity, revealed a significant linear decrease (parameters given in Table S7) in calcification rate with $[\text{Ca}^{2+}]$ (ANCOVA, $F_{(2,54)} = 106.9$, $p < 0.001$) across the range of experimental $[\text{Ca}^{2+}]$ (Fig. 2b). Salinity as a single factor had no significant impact on calcification rates (ANCOVA, $F_{(2,54)} = 0.83$, $P = 0.442$) however, a significant interaction effect between salinity and $[\text{Ca}^{2+}]$ suggests that the effects of $[\text{Ca}^{2+}]$ on calcification rate vary at different salinities. Combining both experiments, calcification rates did not exhibit any significant correlation with $[\text{Ca}^{2+}]$ or $[\text{HCO}_3^-]$ alone under the given conditions (Fig. S4, Table S8). Calcification rates plotted separately against $\Omega_{\text{aragonite}}$ and ESIR across both experiments revealed statistically significant estimations for both parameters (C_{max} and K) in the negative exponential decay model (Fig. 3, Table S6). Estimated model parameters were not significantly different between $\Omega_{\text{aragonite}}$ nor ESIR as calcification predictors, (95 % CI; Fig. S6). Although, a lower residual sum of squares (residual SS = 2866) in the ESIR model compared to the $\Omega_{\text{aragonite}}$ model (residual SS = 3159) indicates slightly better performance of the ESIR model as a predictor for calcification in the southwest and Central Baltic Sea. Despite different aquarium volumes and animal numbers per replicate, calcification rates were comparable between both laboratory experiments (Fig. 2). Field calcification rates were also comparable with laboratory experiments, at least for Ahrenshoop (mean salinity: 10.9) and Usedom (mean salinity: 7.0) populations (Table 3). Mussels from Kiel (mean salinity: 15.2) exhibited significantly higher calcification rates (ANCOVA, $F_{(2,12)} = 570$, $P < 0.001$) compared to the two other field sites, being 1-2 orders of magnitude higher (Fig. 4). This contrasts with measured laboratory calcification rates where salinities 16 and 11 treatments exhibited comparable calcification rates ($\mu\text{g CaCO}_3 \text{ d}^{-1}$).

3.2 Environmental monitoring

290 Salinity was different between all three monitoring sites (ANCOVA, $F_{(2, 17253)} = 38518$, $p < 0.001$, Table S6) being highest and more variable in Kiel and lowest and the most stable in Usedom (Fig. 5). As salinity and $[\text{Ca}^{2+}]$ exhibit a linear relationship (Fig. S2), $[\text{Ca}^{2+}]$ also differed to the same degree as salinity between the three sites (Fig. 5). Calculated mean $[\text{HCO}_3^-]$ at the three field sites (Table 3) were significantly higher in Kiel compared to Ahrenshoop and Usedom (ANOVA, $F_{(2, 55)} = 38.80$, $p < 0.001$, Table S6) with values never dropping below 1600 $\mu\text{mol kg}^{-1}$ at any of the three sites during the monitoring period (Fig. 6c). While pH was highly variable,



particularly in Kiel (Fig. 6a), no difference was observed between all 3 sites (ANOVA, $F_{(2,55)} = 1.217$, $p = 0.304$). Salinity and A_T exhibited a linear association similar in slope to the S - A_T relationship reported by Müller, et al., 2016 for the Kattegat in 2014 (Fig. 7). However, A_T values measured in this study were ca. $100 \mu\text{mol kg}^{-1}$ higher at a given salinity than those reported by Müller, et al., 2016 for the Kattegat and Central Baltic Proper (model parameters given in Table S9). Calculated $\Omega_{\text{aragonite}}$ was higher in Kiel compared to the other two sites (ANOVA, $F_{(2, 55)} = 7.22$, $p = 0.002$, Fig. 6e) with periods above and below $\Omega_{\text{aragonite}} = 1$ in Kiel (mean = 1.17) and mean values below saturation ($\Omega < 1$) in Ahrenshoop or Usedom at 0.83 and 0.76, respectively (Fig. 6e, Table 3). Similar patterns were observed in the calculated values for ESIR at the three sites (Fig. 6g) with Kiel exhibiting significantly higher mean ESIR values than both Ahrenshoop and Usedom (ANOVA $F_{(2, 55)} = 10.88$, $p < 0.001$), with a mean value of 1.05 ± 0.6 (Table 3). Mean ESIR values were below the threshold of 0.7 proposed by Thomsen, et al., 2018 in Ahrenshoop and Usedom (means of 0.65 ± 0.19 and 0.55 ± 0.26 , respectively; Fig. 6g), although periods above and below this threshold were observed at all sites (Fig. 6g). Mean chl-*a* concentrations at each site (Fig. 6i, Table 3) derived from monitoring data were significantly lower at Ahrenshoop compared to Kiel and Usedom (ANOVA, $F_{(2, 77)} = 13.8$, $p < 0.001$, Table S6) and not significantly different between Kiel and Usedom (Tukey *post-hoc*, $p = 0.35$).

4. Discussion

4.1 Carbonate chemistry

This study aimed to investigate the mechanisms by which low salinity negatively impacts calcification in Baltic mussels. Calcification relies on the uptake of both calcium and inorganic carbon from seawater to precipitate CaCO_3 crystals, and in the low saline southwest Baltic Sea, the availability of both substrates is significantly lower than in the North Sea (Kremling and Wilhelm, 1997; Müller, et al., 2016). The laboratory experiments presented in this study demonstrate that HCO_3^- availability begins to limit calcification below $\sim 1000 \mu\text{mol kg}^{-1}$ (Fig. 2a), in line with similar experiments on *Mytilus edulis* juveniles (Thomsen, et al., 2015). This corresponds to an A_T of $\sim 1050 \mu\text{mol kg}^{-1}$ (at the experimental pH of 7.71). Such low $[\text{HCO}_3^-]$ are unlikely under fully marine conditions, due to high and stable A_T in ocean waters of $\sim 2300 \mu\text{mol kg}^{-1}$ (Millero, et al., 1998). However, estuarine and brackish water environments are often characterised by low A_T due the linear relationship between salinity and A_T , and characteristically have a weaker pH buffering capacity and lower availability of inorganic carbon (Miller, et al., 2009). Despite the low salinity, the Baltic Sea regionally exhibits relatively high A_T due to high riverine A_T from the southern drainage basin (Beldowski, et al., 2010; Müller, et al., 2016). Monitoring results from three coastal sites in the southwest Baltic revealed higher values of A_T for a given salinity, than would be expected based on the 2014 S - A_T relationship presented in Müller, et al., 2016 (Fig. 7). As samples were taken in direct proximity to the coastline, this is likely due to mixing of local freshwater endmembers (either rivers or submarine groundwater discharge). Local freshwater endmembers in the southern drainage basin are known to have a higher A_T than the mean volume-weighted Baltic Sea freshwater endmember, which is reduced by the influence of low A_T rivers in Scandinavia (Müller, et al., 2016). The proximity to the southern coastline and higher fraction of freshwater from the southern drainage basin likely explains the offset of the A_T - S relationships from our monitoring sites with respect to the relationships reported by e.g Müller, et al., 2016. Dissolved organic carbon (DOC) species also constitute 1.5-2.3 % of A_T in the southwest and Central Baltic, and DOC from the Oder river discharge may contribute to the high coastal A_T observed in the southwest Baltic in this study (Kuliński, et al., 2014). The high A_T observed across all sites in this study (1856 - $2071 \mu\text{mol kg}^{-1}$) suggests that HCO_3^- limitation at A_T values $< 1050 \mu\text{mol kg}^{-1}$ is likely not the primary reason for reduced calcification in Baltic mussels.

It is not possible to disentangle the effects of inorganic carbon availability from pH in the bicarbonate limitation experiment. This is because the methodologies applied in this study of manipulating $[\text{HCO}_3^-]$ meant reducing A_T in parallel and consequently lowering seawater pH as pCO_2 remained unchanged (Table 1). Reduced seawater pH through experimentally increasing pCO_2 , has been demonstrated to reduce calcification rates in bivalve larvae and coral due to alteration of optimum proton gradients between seawater and the site of calcification (Allison, et al., 2014; Ramesh, et al., 2017). Although, experiments utilising methods which manipulate individual parameters of the carbonate system have suggested pH as a sole parameter does not correlate strongly with molluscan calcification when compared to SIR, $[\text{CO}_3^{2-}]$ and $\Omega_{\text{aragonite}}$ (Waldbusser, et al., 2014; Thomsen, et al., 2015). Since marine organisms modify the carbonate chemistry at the site of calcification, it is not possible to differentiate between the effects of Ω on net CaCO_3 dissolution or reduced crystal nucleation and the effects of physiological alterations of the carbonate chemistry in the calcifying space (Cyronak, et al., 2016; Ramesh, et al., 2017). Calcification is stimulated by the availability of calcification substrate (Ca^{2+} and HCO_3^-) and inhibited by H^+ , therefore the application of the SIR provides a more physiologically oriented predictor of calcification. However, the nature of the carbonate system results in the SIR co-correlating strongly with both $[\text{CO}_3^{2-}]$ and Ω at a constant salinity, temperature and pressure (Bach, 2015; Thomsen, et al., 2015; Cyronak, et al., 2016; Fassbender, et al., 2016).



In our experiments the classical SIR ($[\text{HCO}_3^-]/[\text{H}^+]$) proved to be a poor predictor of calcification (Fig. S5) in comparison to $\Omega_{\text{aragonite}}$ (Fig. 3a) when $[\text{Ca}^{2+}]$ was experimentally manipulated. Building on the findings from the HCO_3^- limitation experiment, this experiment individually isolated the impacts of salinity and $[\text{Ca}^{2+}]$ revealing that salinity as a sole factor had no significant impact on calcification rates, whilst $[\text{Ca}^{2+}]$ correlated linearly with calcification across all $[\text{Ca}^{2+}]$. This suggests Ca^{2+} to be the limiting factor for calcification at concentrations < 4 mmol kg^{-1} or corresponding to a salinity of ~ 11 on the natural salinity gradient, in line with previous studies on Baltic mussel larvae and adults (Kossak, 2006; Sanders, et al., 2018; Thomsen, et al., 2018). Negative exponential decay models did not return significant parameter estimations for C_{max} (maximum calcification rates) in the calcium experiment as in the bicarbonate experiment (Table S7). This indicates that threshold values of $[\text{Ca}^{2+}]$ saturation for calcification (above which calcification rate is unaffected by further increases in $[\text{Ca}^{2+}]$) are higher than the maximum experimental levels here (ca. 3.8 mmol kg^{-1}). A threshold of ~ 4 mmol kg^{-1} for calcification has been observed for larvae and seems to be comparable for juveniles as well (Thomsen et al., 2018). Further experiments spanning a wider range of $[\text{Ca}^{2+}]$ eg. 0.5-8 mmol kg^{-1} , may reveal significant effects of salinity on calcification when $[\text{Ca}^{2+}] > 4$ mmol kg^{-1} . The significant interaction effect between salinity and $[\text{Ca}^{2+}]$ on calcification in the calcium experiment (Table S6) may hint that salinity has a stronger impact on calcification at higher and non-limiting $[\text{Ca}^{2+}]$. Reduced calcification rates at salinities < 11 were also observed in the field with mussels at Ahrenshoop and Usedom exhibiting significantly reduced calcification compared to Kiel (Fig. 4). As a single factor, $[\text{Ca}^{2+}]$ was a poor predictor of calcification across both laboratory experiments (Fig. S4a). However, in this study, extending the SIR (ESIR) to include $[\text{Ca}^{2+}]$ as a substrate yielded a significant relationship with calcification, in line with $\Omega_{\text{aragonite}}$ as a calcification predictor (Fig. 3). Accounting for $[\text{Ca}^{2+}]$ in the ESIR model is likely only necessary at salinities ≤ 11 when Ca^{2+} availability starts to become limiting (Thomsen, et al., 2018). There was no statistically significant difference between both ESIR and $\Omega_{\text{aragonite}}$ models as calcification predictors in this study which may result from the low values of both in the Baltic Sea. $\Omega_{\text{aragonite}}$ is particularly low in winter when low temperatures (Fig. S7) and high pCO_2 from upwelling and water mixing, increase K_{sp} and decrease $[\text{CO}_3^{2-}]$, respectively, Eq. (1). Salinity and temperature also impact aragonite saturation state ($\Omega_{\text{aragonite}}$) due to the salinity and temperature dependant nature of the solubility product of aragonite, K_{sp} , Eq. (1) and the CO_2 dissociation constants. Conversely, temperature has almost no impact on ESIR when salinity and pressure are constant (see Bach, 2015). ESIR is also unimpacted by salinity *per se*, but rather $[\text{Ca}^{2+}]$ which correlates with salinity, although future trends in the S- Ca^{2+} relationship in the southwest and Central Baltic may deviate from current relationships (see section 4.5). Both ESIR and Ω generally correlate well in marine systems, however this linear relationship is skewed in coastal zones where variability in carbonate chemistry parameters is high (Fassbender, et al., 2016). This is highlighted in Fig. S8, where a given $\Omega_{\text{aragonite}}$ of 1.0 can correspond to ESIR values of between 0.5-1.3 (well above and below the limiting ESIR threshold of 0.7). ESIR and $\Omega_{\text{aragonite}}$ are certainly stronger predictors of calcification than calcification substrate availability alone in the southwest Baltic. However, the strong interdependency between both parameters makes it impossible to differentiate one from the other as a more powerful predictor of calcification in this study.

4.2 Physiology

Reduced calcification rates under sub-optimal carbonate chemistry conditions in this study may be explained in terms of calcification physiology. Adult bivalve molluscs are poor at regulating the ion composition of their extracellular fluid, thus low seawater $[\text{Ca}^{2+}]$ directly translates to low haemolymph $[\text{Ca}^{2+}]$ with the same concept applying to seawater pCO_2 , pH and $[\text{HCO}_3^-]$. However extracellular carbonate chemistry is even less favourable for calcification than ambient seawater as production of metabolic CO_2 maintains extracellular pCO_2 higher than ambient seawater to aid diffusive excretion of metabolic CO_2 (Melzner, et al., 2009; Heinemann, et al., 2012). Sub-optimal carbonate chemistry in the extracellular fluid will therefore be in direct contact with the mantle epithelia (calcifying tissue) and likely impact energy demanding ion transport processes involved in calcification. At a cellular level, low seawater Ca^{2+} availability may impact calcification by reduced rates of calcium transport across the mantle epithelia by plasma membrane Ca^{2+} ATPases (PMCA) (Niggli, 1982; McConnaughey and Whelan, 1997). Although PMCA activity and gene expression has not been shown to be impacted by salinity in *Mercenaria mercenaria* and *Crassostrea gigas*, respectively, actual rates of Ca^{2+} transport across the mantle epithelia have been shown to decrease at salinities of 14 compared to 28 in *C. gigas* (Ivanina, et al., 2020; Sillanpää, et al., 2020). This suggests that the reduced calcification rates observed in this study at low $[\text{Ca}^{2+}]$ may stem from a reduced supply of Ca^{2+} to the calcification site. Conversely, protons (H^+) inhibit calcification in the calcifying space by lowering Ω and imposing constraints on mineral formation (Waldbusser, et al., 2014; Cyronak, et al., 2016). Organisms may increase the rate of H^+ extrusion from the calcifying space (via the V-type H^+ -ATPase) but this requires more energy in the form of ATP, increasing calcification costs and potentially resulting in less energy available for other processes eg. protein synthesis (Waldbusser, et al., 2013; Tresguerres, 2016). Higher energetic costs of calcification have been documented at low salinities (Sanders et al., 2018) and this may be the underlying mechanisms explaining the reduced calcification rates at low salinities and $[\text{Ca}^{2+}]$.



4.3 Salinity

Salinity is known to have a strong impact on bivalve growth and survival in the Baltic Sea, particularly at salinities ≤ 11 (Kautsky, et al., 1990; Kossak, 2006; Riisgård, et al., 2014; Sanders, et al., 2018). It has long been assumed that the underlying physiological mechanism stems from intracellular osmotic stress at low salinities and inefficient protein metabolism (Tedengren and Kautsky, 1986; Maar, et al., 2015). However recent work suggests that a reduced ability to biomineralize CaCO_3 may be limiting growth rates at low salinities, rather than inefficient growth associated with osmotic stress (Riisgård, et al., 2014; Sanders, et al., 2018; Thomsen, et al., 2018; Sillanpää, et al., 2020). In this study, salinity had a significant effect on calcification in the bicarbonate limitation experiment but when decoupled from $[\text{Ca}^{2+}]$ in the following experiment, salinity as a single factor did not impact calcification and overall growth. The observed interaction effect on calcification between $[\text{Ca}^{2+}]$ and salinity suggests the impacts of salinity cannot be excluded, and at saturated calcium concentrations ($> 4 \text{ mmol kg}^{-1}$), the individual impacts of salinity on growth may be more apparent. The metabolic costs associated with osmotic stress result from cellular mechanisms of volume control during salinity changes (Neufeld, et al., 1996). Intracellular organic osmolytes (primarily free amino acids and quaternary ammonium compounds) are cellularly excreted or mobilised from endogenous protein reserves during hypo- and hyper-salinity exposure, respectively (Hawkins and Hilbish, 1992). Once long term (> 2 weeks) acclimation to salinity changes have been made, it is not clear what, if any, metabolic costs persist. Both laboratory experiments in this study lasted > 30 days, long enough to overcome the initial energetic costs of salinity acclimation. Accordingly, the results here suggest that at salinities between 7-16, osmotic stress is not the primary cause of reduced calcification rates and growth in Baltic mussels.

4.4 Field conditions

Both ESIR and $\Omega_{\text{aragonite}}$ values were almost permanently below critical thresholds and saturation levels, respectively, in Ahrenshoop and Usedom and extended periods of undersaturation were observed in Kiel Fjord. Yet despite these conditions, net positive calcification rates were recorded at all sites with mussels in Kiel Fjord exhibiting calcification rates 1-2 orders of magnitude higher than the two low salinity sites. This is interesting, as extremely low and variable pH (Fig. 6b) and other carbonate chemistry parameters have been well documented in Kiel Fjord with extended periods of Ω undersaturation, particularly in early autumn during seasonal upwelling of hypercapnic water (Thomsen, et al., 2010; Melzner, et al., 2013; Saderne, et al., 2013). These drastically higher rates of calcification in Kiel Fjord are unlikely to result solely from high ESIR and $\Omega_{\text{aragonite}}$ values, as the laboratory experiments in this study clearly reveal minor differences in calcification rates above and below ESIR saturation (see Fig. 3), compared to field calcification rates. It is more probable that the high levels of eutrophication in Kiel Fjord and consequently high phytoplankton food concentrations are responsible for the rapid calcification observed in this study (Melzner, et al., 2011; Thomsen, et al., 2013). Chl-*a* monitoring data in this study partially supports this with mean values in Kiel significantly higher than Ahrenshoop. However, chl-*a* values in Usedom (low salinity) were comparable with Kiel despite drastically lower calcification rates in Usedom. Two-fold differences in particulate organic carbon (POC), have been documented between the inner and outer Kiel Fjord which presumably lead to higher phytoplankton abundance and food availability in the inner Fjord and resulting higher calcification rates (Thomsen, et al., 2013). The growth monitoring site of this study was also located in the inner Fjord, however chl-*a* measurements were taken in the outer Fjord and subsequently may not be fully representative of the Kiel mussel monitoring site. Values for chl-*a* and food availability to inner Kiel Fjord mussels may in fact be significantly higher than reported here, which likely explains the extremely high growth rates in Kiel compared to the other two monitoring sites. Conversely, the fact that calcification rates in Usedom were considerably lower than Kiel is likely due to limited $[\text{Ca}^{2+}]$ and sub-optimal ESIR values. It may be that increased energy uptake in the form of phytoplankton food cannot compensate for this substrate limitation. This is contrary to laboratory findings by Thomsen, et al., 2013, where higher food availability could mediate the adverse effects of high pCO_2 and low pH on calcification rates. The laboratory experiments presented here indicate calcification rates decrease linearly when $[\text{Ca}^{2+}] < 4 \text{ mmol kg}^{-1}$ and monitoring data revealed mean $[\text{Ca}^{2+}]$ at Ahrenshoop and in particular Usedom to be well below 4 mmol kg^{-1} , but not in Kiel (Fig. 5). Although pH is intrinsically linked to both Ω and ESIR, mean pH_{total} values were not different between the 3 sites (Fig. 6a) despite significant differences between Ω and ESIR. $[\text{HCO}_3^-]$ was $\sim 10\%$ lower in Ahrenshoop and Usedom compared to Kiel, whereas $[\text{Ca}^{2+}]$ was 22% and 48% lower in Ahrenshoop and Usedom than in Kiel, respectively. This suggests low calcification rates at salinities ≤ 11 in the southwest Baltic result from low ESIR or Ω values primarily due to low seawater Ca^{2+} availability, rather than high $[\text{H}^+]$ and low $[\text{HCO}_3^-]$ (Fig. S9).

4.5 Future trends

Desalination of the southwest and Central Baltic Proper is projected over the next century due to increased freshwater supply from river discharge resulting from changes in precipitation patterns (Meier, et al., 2006; Gräwe, et al., 2013). Depending on the composition of the additional freshwater input, this desalination might also suggest a reduction in A_T and $[\text{Ca}^{2+}]$, however A_T has in fact increased in the Central Baltic Sea by $\sim 3.4 \mu\text{mol}$



480 $\text{kg}^{-1} \text{yr}^{-1}$ over the past two decades likely due to changes in precipitation and continental weathering (Müller, et al., 2016), which has also increased $[\text{Ca}^{2+}]$ and $\text{Ca}-A_T$ ratios over a similar time period (Kremling and Wilhelm, 1997). Although future changes in A_T and $[\text{Ca}^{2+}]$ may be unclear at present, the magnitude of predicted desalination, coupled with projected reduction in eutrophication and increasing atmospheric pCO_2 points towards a trend of decreasing pH in the Central Baltic Sea over the next century (Gustafsson, et al., 2019; Gustafsson and Gustafsson, 2020). Future acidification combined with a potential mismatch in future $\text{S}-\text{Ca}^{2+}$ relationships highlight the importance of utilising ESIR over Ω in predicting vulnerability of marine calcifiers in the southwest and Central Baltic Sea. In the absence of adaptation, projected environmental change may result in a westward distribution shift of marine calcifying mussels towards the Kattegat, and/or replacement of calcifying mytilid mussels in the southwest and Central Baltic by brackish or freshwater calcifying bivalves such as the invasive euryhaline freshwater bivalve, *Dreissena* spp. These changes may have potential knock-on effects for benthic biodiversity and nutrient recycling in the southwest and Central Baltic Sea (Vuorinen, et al., 2015).

5. Conclusions

490 The environmental gradients in the Baltic Sea provide an excellent system to investigate the impacts of seawater carbonate chemistry on marine calcifying organisms. The results presented here show that extremely slow calcification rates in the Baltic Sea arise from extended periods of $\Omega_{\text{aragonite}}$ and ESIR undersaturation. These sub-optimal conditions for calcification arise primarily from low seawater $[\text{Ca}^{2+}]$ rather than low $[\text{HCO}_3^-]$ and low pH. Although high food availability and high A_T near the coast may alleviate these negative impacts at salinities > 11 , this is likely not possible when $[\text{Ca}^{2+}]$ is ultimately limiting calcification $< 4 \text{ mm kg}^{-1}$. Predicted acidification and desalination in the southwest Baltic is likely to impact Baltic *Mytilus* calcification and distributions, however this will depend on future $[\text{Ca}^{2+}]$ trends. Upcoming work investigating the impacts of climate change on Baltic Sea calcifying organisms should a) focus on better understanding future changes in $[\text{Ca}^{2+}]$ in the southwest and Central Baltic Proper and b) further investigate the mechanisms and costs associated with cellular Ca^{2+} transport in bivalves and assess their potential to adapt their calcification machinery to future Baltic Sea conditions.

Data availability

All raw data is available via the Pangaea database (doi: *data submission pending*).

505 Author contributions

TS, FM and JT designed the laboratory experiments conducted by TS and JT. TS, FM, GR and JDM implemented the environmental monitoring and TS collected and analysed environmental data. JDM and GR analysed carbonate chemistry samples. TS wrote the manuscript with all authors providing significant contributions throughout.

510

Competing interests

The authors declare no conflict of interest.

Acknowledgements

515 The authors thank Stefan Otto at the IOW for carbonate chemistry analysis of samples and Thomas Stegmann at the Christian Albrechts Universität zu Kiel for Ca^{2+} measurements. The authors also thank the Landesamt für Landwirtschaft, Umwelt und Ländliche Räume (LLUR, Kiel) and the Landesamt für Umwelt, Naturschutz und Geologie (LUNG, Güstrow) for chl-*a* monitoring data. Additionally, the authors would like to thank Luca Telesca (Cambridge University) for assisting the analysis of environmental data. This research was supported by the Marie Curie ITN network ‘CACHE’ (Calcium in a Changing Environment), European Union Seventh Framework Programme under grant agreement n° 605051. The position of JDM was funded by BONUS, the joint Baltic Sea research and development programme (Art 185), funded jointly from the European Union’s Seventh Programme for research, technological development and demonstration and from the German Federal Ministry of Education and Research through Grant No. 03F0689A (BONUS PINBAL) and Grant No. 03F0773A (BONUS INTEGRAL).

525

References

Allison, N., Cohen, I., Finch, A. A., Erez, J., Tudhope, A. W. and Edinburgh Ion Microprobe Facility.: Corals concentrate dissolved inorganic carbon to facilitate calcification, *Nat. Commun.*, 5, 5741, <https://doi.org/10.1038/ncomms6741>, 2014

530

Bach, L. T.: Reconsidering the role of carbonate ion concentration in calcification by marine organisms, *Biogeosciences*, 12, 4939-4951, <https://doi.org/10.5194/bg-12-4939-2015>, 2015.



- 535 Beldowski, J., Löffler, A., Schneider, B. and Joensuu, L.: Distribution and biogeochemical control of the total CO₂ and total alkalinity in the Baltic Sea, *J. Marine Syst.*, 81, 252–259, <https://doi.org/10.1016/j.jmarsys.2009.12.020>, 2010.
- Cyronak, T., Schulz, K. G. and Jokiel, P. L.: The Omega myth: what really drives lower calcification rates in an acidifying ocean. *ICES J. Mar. Sci.*, 73, 558–562, <https://doi.org/10.1093/icesjms/fsv075>, 2016.
- 540 Dickson, A. G.: Standard potential of the reaction $-AgClS+1/2 H_2 = AgS+HClAq$ and the standard acidity constant of the ion HSO₄⁻ in synthetic sea-water from 273.15-K to 318.15-K, *J. Chem. Thermodyn.*, 22, 113–127, [https://doi.org/10.1016/0021-9614\(90\)90074-Z](https://doi.org/10.1016/0021-9614(90)90074-Z), 1990.
- 545 Dickson, A. G., Afgan, J. D. and Anderson, G. C.: Reference materials for oceanic CO₂ analysis: a method for the certification of total alkalinity, *Mar. Chem.*, 80, 185–197, [https://doi.org/10.1016/S0304-4203\(02\)00133-0](https://doi.org/10.1016/S0304-4203(02)00133-0), 2003.
- Dickson, A. G., Sabine, C. L. and Christian, J. R.: Guide to best practices for ocean CO₂ measurements, *PICES Special Publication*, 3, 191 pp, 2007.
- 550 EU, Copernicus Marine Service.: Copernicus Marine Environment Monitoring Service – CMEMS, 2018. Available at: <http://marine.copernicus.eu/>, accessed 7th February 2018.
- 555 Fassbender, A. J., Sabine, C. L. and Feifel, K. M.: Consideration of coastal carbonate chemistry in understanding biological calcification, *Geophys. Res. Lett.*, 43, 4467–4476, <https://doi.org/10.1002/2016GL068860>, 2016.
- Gräwe, U., Friedland, R. and Burchard, H.: The future of the western Baltic Sea: two possible scenarios, *Ocean Dyn.*, 63, 901–921, <https://doi.org/10.1007/s10236-013-0634-0>, 2013.
- 560 Gustafsson, E., Hagens, M., Sun, X., Reed, D. C., Humborg, C., Slomp, C. P., and Gustafsson, B. G.: Sedimentary alkalinity generation and long-term alkalinity development in the Baltic Sea, *Biogeosciences*, 16, 437–456, <https://doi.org/10.5194/bg-16-437-2019>, 2019.
- 565 Gustafsson, E. and Gustafsson, Bo. G.: Future acidification of the Baltic Sea – A sensitivity study, *J. Marine Syst.*, 211, 103397, <https://doi.org/10.1016/j.jmarsys.2020.103397>, 2020.
- 570 Hammer, K., Schneider, B., Kuliński, K. and Schulz-Bull, D. E.: Precision and accuracy of spectrophotometric pH measurements at environmental conditions in the Baltic Sea, *Estuar. Coast. Shelf Sci.*, 146, 24–32, <https://doi.org/10.1016/j.ecss.2014.05.003>, 2014.
- Hawkins, A. J. S. and Hilbish, T. J.: The cost of cell volume regulation: protein metabolism during hyperosmotic adjustment, *J. Mar. Biol. Assoc. U.K.*, 72, 569–578, <https://doi.org/10.1017/S002531540005935X>, 1992.
- 575 HELCOM.: Eutrophication status of the Baltic Sea 2007–2011 – A concise thematic assessment, *Baltic Sea Environmental Proceedings No. 143*, 2014.
- 580 Heinemann, A., Fietzke, J., Melzner, F., Böhm, F., Thomsen, J., Garbe-Schönberg, D. and Eisenhauer, A.: Conditions of *Mytilus edulis* extracellular body fluids and shell composition in a pH-treatment experiment: Acid-base status, trace elements and δ¹¹B, *Geochim. Geophys. Geosy.*, 13, Q01005, <https://doi.org/10.1029/2011GC003790>, 2012.
- 585 Hiebenthal, C., Fietzke, P., Müller, J. D., Otto, S., Rehder, G., Paulsen, M., Stühr, A., Clemmesen, C. and Melzner, F.: Kiel Fjord carbonate chemistry data between 2015 (January) and 2016 (January), *GEOMAR – Helmholtz Centre for Ocean Research Kiel, PANGAEA*, <https://doi.org/10.1594/PANGAEA.876551>, 2017.
- 590 Hjerne, O., Hajdu, S., Larsson, U., Downing, A. S. and Winder, M.: Climate driven changes in timing, composition and magnitude of the Baltic Sea phytoplankton spring bloom, *Front. Mar. Sci.*, 6, 482, <https://doi.org/10.3389/fmars.2019.00482>, 2019.
- Hu, H. Y., Yan, J.-J., Petersen, I., Himmerkus, N., Bleich, M., Stumpp, M.: A SLC4 family bicarbonate transporter is critical for intracellular pH regulation and biomineralization in sea urchin embryos, *eLife*, 7, e36600, <https://doi.org/10.7554/eLife.36600.001>, 2018.



- 595 Ivanina, A. V., Jarrett, A., Bell, T., Rimkevicius, T., Beniash, E. and Sokolova, I. M.: Effects of seawater salinity and pH on cellular metabolism and enzyme activities in biomineralizing tissues of marine bivalves, *Comp. Biochem. Physiol. Part A Mol. Integr. Physiol.*, 248, 110748, <https://doi.org/10.1016/j.cbpa.2020.110748>, 2020.
- 600 Jokiel, P. L.: Coral reef calcification: carbonate, bicarbonate and proton flux under conditions of increasing ocean acidification, *P. Roy. Soc. B*, 280, 20130031, <https://doi.org/10.1098/rspb.2013.0031>, 2013.
- Kautsky, N., Johannesson, K. and Tedengren, M.: Genotypic and phenotypic differences between Baltic and North Sea populations of *Mytilus edulis* evaluated through reciprocal transplantations. I. Growth and morphology, *Mar. Ecol. Prog. Ser.*, 59, 203–210, <https://doi.org/10.3354/meps059203>, 1990.
- 605 Kester, D. R., Duedall, I. W., Connors, D. N. and Pytkowicz, R. M.: Preparation of artificial seawater, *Limnol. Oceanogr.*, 12, 176-179, <https://doi.org/10.4319/lo.1967.12.1.0176>, 1967.
- 610 Kossak, U.: How climate change translates into ecological change: Impacts of warming and desalination on prey properties and predator-prey interactions in the Baltic Sea, PhD Thesis: Mathematics and Natural Sciences faculty of Christian Albrechts University, Kiel, 2006.
- Kotta, J., Futter, M., Kaasik, A., Liversage, K., Rätsep, M., Barboza, F. R., Bergström, L., Bergström, P., Bobsien, I., Díaz, E., Herkül, K., Jonsson, P. R., Korpinen, S., Kraufvelin, P., Krost, P., Lindahl, O., Lindegarth, M., Lyngsgaard, M. M., Mühl, M., Sandman, A. N., Orav-Kotta, H., Orlova, M., Skov, H., Rissanen, J., Šiaulyš, A., Vidakovic, A. and Virtanen, E.: Cleaning up seas using blue growth initiatives: Mussel farming for eutrophication control in the Baltic Sea, *Sci. Total Environ.*, 709, 136144, <https://doi.org/10.1016/j.scitotenv.2019.136144>, 2020.
- 620 Kremling, K. and Wilhelm, G.: Recent increase of the calcium concentrations in Baltic Sea waters, *Mar. Pollut. Bull.*, 34, 763-767, [https://doi.org/10.1016/S0025-326X\(97\)00048-9](https://doi.org/10.1016/S0025-326X(97)00048-9), 1997.
- Kuliński, K., Schneider, B., Hammer, K., Machulik, U. and Schulz-Bull, D.: The influence of dissolved organic matter on the acid-base system of the Baltic Sea, *J. Marine Syst.*, 132, 106-115, <https://doi.org/10.1016/j.jmarsys.2014.01.011>, 2014.
- 625 Maar, M., Saurel, C., Landes, A., Dolmer, P. and Petersen, J. K.: Growth potential of blue mussels (*M. edulis*) exposed to different salinities evaluated by a Dynamic Energy Budget model, *J. Marine Syst.*, 148, 48-55, <https://doi.org/10.1016/j.jmarsys.2015.02.003>, 2015.
- 630 McConnaughey, T. A. and Whelan, J. F.: Calcification generates protons for nutrient and bicarbonate uptake, *Earth-Sci. Rev.*, 42, 95-117, [https://doi.org/10.1016/S0012-8252\(96\)00036-0](https://doi.org/10.1016/S0012-8252(96)00036-0), 1997.
- 635 Meier, H. E. M.: Baltic Sea climate in the late twenty-first century: a dynamical downscaling approach using two global models and two emission scenarios, *Clim. Dyn.*, 27, 39-68, <https://doi.org/10.1007/s00382-006-0124-x>, 2006.
- Melzner, F., Gutowska, M. A., Langenbuch, M., Dupont, S., Lucassen, M., Thorndyke, M. C., Bleich, M. and Pörtner, H. O.: Physiological basis for high CO₂ tolerance in marine ectothermic animals: pre-adaptation through lifestyle and ontogeny?, *Biogeosciences*, 6, 2313–2331, <https://doi.org/10.5194/bg-6-2313-2009>, 2009.
- 640 Melzner, F., Stange, P., Trübenbach, K., Thomsen, J., Casties, I., Panknin, U., Gorb, S. N. and Gutowska, M.: Food supply and seawater pCO₂ impact calcification and internal shell dissolution in the blue mussel *Mytilus edulis*, *PLoS ONE*, 6, e24223, <https://doi.org/10.1371/journal.pone.0024223>, 2011.
- 645 Melzner, F., Thomsen, J., Koeve, W., Oschlies, W., Gutowska, M. A., Bange, H. W., Hansen, H. P. and Körtzinger, A.: Future ocean acidification will be amplified by hypoxia in coastal habitats, *Mar. Biol.*, 160, 1875-1888, <https://doi.org/10.1007/s00227-012-1954-1>, 2013.
- 650 Miller, A. W., Reynolds, A. C., Sobrino, C. and Riedel, G. F.: Shellfish face uncertain future in high CO₂ world: Influence of acidification on oyster larvae calcification and growth in estuaries, *PLoS ONE*, 4, E5661, <https://doi.org/10.1371/journal.pone.0005661>, 2009.



- 655 Millero, F.: The conductivity-density-salinity-chlorinity relationships for estuarine water, *Limnol. Oceanogr.*, 29, 1317–1321, <https://doi.org/10.4319/lo.1984.29.6.1317>, 1984.
- 660 Millero, F. J., Lee, K. and Roche, M.: Distribution of alkalinity in the surface waters of the major oceans, *Mar. Chem.*, 60, 111-130, [https://doi.org/10.1016/S0304-4203\(97\)00084-4](https://doi.org/10.1016/S0304-4203(97)00084-4), 1998.
- 665 Millero, F. J.: Carbonate constants for estuarine waters, *Mar. Freshwater Res.*, 61, 139-142, <https://doi.org/10.1071/MF09254>, 2010.
- 670 Mohrholz, V., Naumann, M., Nausch, G., Krüger, S. and Gräwe, U.: Fresh oxygen for the Baltic Sea – an exceptional saline inflow after a decade of stagnation, *J. Marine Syst.* 148, 152-166, <https://doi.org/10.1016/j.jmarsys.2015.03.005>, 2015.
- 675 Müller, J. D., Schneider, B. and Rehder, G.: Long-term alkalinity trends in the Baltic Sea and their implications for CO₂-induced acidification, *Limnol. Oceanogr.*, 61, 1984-2002, <https://doi.org/10.1002/lno.10349>, 2016.
- 680 Müller, J. D. and Rehder, G.: Metrology of pH Measurements in Brackish Waters—Part 2: Experimental Characterization of Purified meta-Cresol Purple for Spectrophotometric pH Measurements, *Front. Mar. Sci.*, 5, 177, <https://doi.org/10.3389/fmars.2018.00177>, 2018.
- 685 Neufeld, D. S. and Wright, S. H.: Response of cell volume in *Mytilus* gill to acute salinity change, *J. Exp. Biol.*, 199, 473-484, 1996.
- 690 Neumann, T.: Climate-change effects on the Baltic Sea ecosystem: A model study, *J. Marine Syst.*, 81, 213-224, <https://doi.org/10.1016/j.jmarsys.2009.12.001>, 2010.
- 695 Niggli, V., Sigel, E. and Carafoli, E.: The purified Ca²⁺ pump of human erythrocyte membranes catalyzes an electroneutral Ca²⁺-H⁺ exchange in reconstituted liposomal systems, *JBC*, 257, 2350-2356, [https://doi.org/10.1016/0143-4160\(82\)90010-0](https://doi.org/10.1016/0143-4160(82)90010-0), 1982.
- 700 Norling, P. and Kautsky, N.: Patches of the mussel *Mytilus* sp. are islands of high biodiversity in subtidal sediment habitats in the Baltic Sea, *Aquat. Biol.*, 4, 75-87, <https://doi.org/10.3354/ab00096>, 2008.
- 705 Ramesh, K., Hu, M. Y., Thomsen, J., Bleich, M. and Melzner, F.: Mussel larvae modify calcifying fluid carbonate chemistry to promote calcification, *Nat. Commun.*, 8, 1709, <https://doi.org/10.1038/s41467-017-01806-8>, 2017.
- 710 Ries, J. B., Ghazaleh, M. N., Connolly, B., Westfiel, I. and Castillo, K. D.: Impacts of seawater saturation state ($\Omega_A = 0.4-4.6$) and temperature (10, 25 °C) on the dissolution kinetics of whole-shell biogenic carbonates, *Geochim. Cosmochim. Acta*, 192, 318-337, <https://doi.org/10.1016/j.gca.2016.07.001>, 2016.
- 715 Riisgård, H. U., Larsen, P. S., Turja, R. and Lundgreen, K.: Dwarfism of blue mussels in the low saline Baltic Sea – growth to the lower salinity limit, *Mar. Ecol. Prog. Ser.*, 517, 181-192, <https://doi.org/10.3354/meps11011>, 2014.
- 720 Roleda, M. Y., Boyd, P. W. and Hurd, C. L.: Before ocean acidification: calcifier chemistry lessons (1), *J. Phycol.*, 48, 840-843, <https://doi.org/10.1111/j.1529-8817.2012.01195.x>, 2012.
- 725 Saderne, V., Fietzek, P. and Herman, P. M. J.: Extreme variations of pCO₂ and pH in a macrophyte meadow of the Baltic Sea in summer: evidence of the effect of photosynthesis and local upwelling, *PLoS ONE*, 8, e62689, <https://doi.org/10.1371/journal.pone.0062689>, 2013.
- 730 Sanders, T., Schmittmann, L., Nascimento-Schulze, J. and Melzner, F.: High calcification costs limit mussel growth at low salinity, *Front. Mar. Sci.*, 5, 352, <https://doi.org/10.3389/fmars.2018.00352>, 2018.
- 735 Sevilgen, D. S., Venn, A. A., Hu, M. Y., Tambutté, E., de Beer, D., Planas-Bielsa, V. and Tambutté, S.: Full in vivo characterization of carbonate chemistry at the site of calcification in corals, *Sci. Adv.*, 16, eaau7447, <https://doi.org/10.1126/sciadv.aau7447>, 2019.



- Sillanpää, J. K., Cardoso, J. C. R., Félix, R. C., Anjos, L., Power, D. M. and Sundell, K.: Dilution of seawater affects the Ca^{2+} transport in the outer mantle epithelium of *Crassostrea gigas*, *Front. Physiol.*, 22, <https://doi.org/10.3389/fphys.2020.00001>, 2020.
- 715 Stuckas, H., Knöbel, L., Schade, H., Breusing, C., Hinrichsen, H. H., Bartel, M., Langguth, C., Melzner, F.: Combining hydrodynamic modelling with genetics: can passive larval drift shape the genetic structure of Baltic *Mytilus* populations? *Mol. Ecol.* 26, 2765-2782, <https://doi.org/10.1111/mec.14075>, 2017.
- 720 Tedengren, M. and Kautsky, N.: Comparative study of the physiology and its probable effect on size in blue mussels (*Mytilus edulis* L.) from the North Sea and the Northern Baltic Proper, *Ophelia*, 25, 147-155, <https://doi.org/10.1080/00785326.1986.10429746>, 1986.
- 725 Thomas, H. and Schneider, B.: The seasonal cycle of carbon dioxide in Baltic Sea surface waters, *J. Marine Syst.*, 22, 53-67, [http://dx.doi.org/10.1016/S0924-7963\(99\)00030-5](http://dx.doi.org/10.1016/S0924-7963(99)00030-5), 1999.
- 730 Thomsen, J., Gutowska, M. A., Saphörster, J., Heinemann, A., Trübenbach, K., Fietzke, J., Hiebenthal, C., Eisenhauer, Körtzinger, A., Wahl, M. and Melzner, F.: Calcifying invertebrates succeed in a naturally CO_2 -rich coastal habitat but are threatened by high levels of future acidification, *Biogeosciences*, 7, 3879-3891, <https://doi.org/10.5194/bg-7-3879-2010>, 2010.
- 735 Thomsen, J., Casties, I., Pansch, C., Körtzinger, A. and Melzner, F.: Food availability outweighs ocean acidification effects in juvenile *Mytilus edulis*: laboratory and field experiments, *Glob. Chang. Biol.*, 19, 1017-1027, <https://doi.org/10.1111/gcb.12109>, 2013.
- 740 Thomsen, J., Ramesh, K., Sanders, T., Bleich, M. and Melzner, F.: Calcification in a marginal sea – Influence of seawater $[\text{Ca}^{2+}]$ and carbonate chemistry on bivalve shell formation, *Biogeosciences*, 15, 1469-1482, <https://doi.org/10.5194/bg-15-1469-2018>, 2018.
- Tresguerres, M.: Novel and potential physiological roles of vacuolar-type H^+ -ATPase in marine organisms, *J. Exp. Biol.* 219, 2088-2097, <https://doi.org/10.1242/jeb.128389>, 2016.
- 745 Tyrrell, T., Schneider, B., Charalampopoulou, A. and Riebesell, U.: Coccolithophores and calcite saturation state in the Baltic and Black Seas, *Biogeosciences*, 5, 485-494, <https://doi.org/10.5194/bg-5-485-2008>, 2008.
- 750 Vuorinen, I., Antsulevich, A. E. and Maximovich, N. V.: Spatial distribution and growth of the common mussel *Mytilus edulis* L. in the archipelago of SW-Finland, northern Baltic Sea, *Boreal Environ. Res.*, 7, 41-52, 2002.
- 755 Vuorinen, I., Hänninen, J., Rajasilta, M., Laine, P., Eklund, J., Montesine-Pouzols, F., Corona, F., Junker, K., Meier, H. E. M. and Dippner, J. W.: Scenario simulations of future salinity and ecological consequences in the Baltic Sea and adjacent North Sea areas – implications for environmental monitoring, *Ecol. Indic.*, 50, 196-205, <https://doi.org/10.1016/j.ecolind.2014.10.019>, 2015.
- 760 Wahl, M., Schneider Covachã, S., Saderne, V., Hiebenthal, C., Müller, J. D., Pansch, C., Sawall, Y.: Macroalgae may mitigate ocean acidification effects on mussel calcification by increasing pH and its fluctuations, *Limnol. Oceanogr.*, 63, 3-21, <https://doi.org/10.1002/lno.10608>, 2017.
- 765 Waldbusser, G. G., Brunner, E. L., Haley, B. A., Hales, B., Langdon, C. J. and Prahl, F. G.: A developmental and energetic basis linking larval oyster shell formation to acidification sensitivity, *Geophys. Res. Lett.*, 40, 2171-2176, <https://doi.org/10.1002/grl.50449>, 2013.
- 770 Waldbusser, G. G., Hales, B., Langdon, C. J., Haley, B. A., Schrader, P., Brunner, E. L., Gray, M. W., Miller, C. A. and Gimenez, I.: Saturation-state sensitivity of marine bivalve larvae to ocean acidification, *Nat. Clim. Chang.*, 5, 273-280, <https://doi.org/10.1038/nclimate2479>, 2014.
- Wasmund, N., Tuimala, J., Suikkanen, S., Vandepitte, L. and Kraberg, A.: Long-term trends in phytoplankton composition in the western and central Baltic Sea, *J. Marine Syst.*, 87, 145-159, <https://doi.org/10.1016/j.jmarsys.2011.03.010>, 2011.

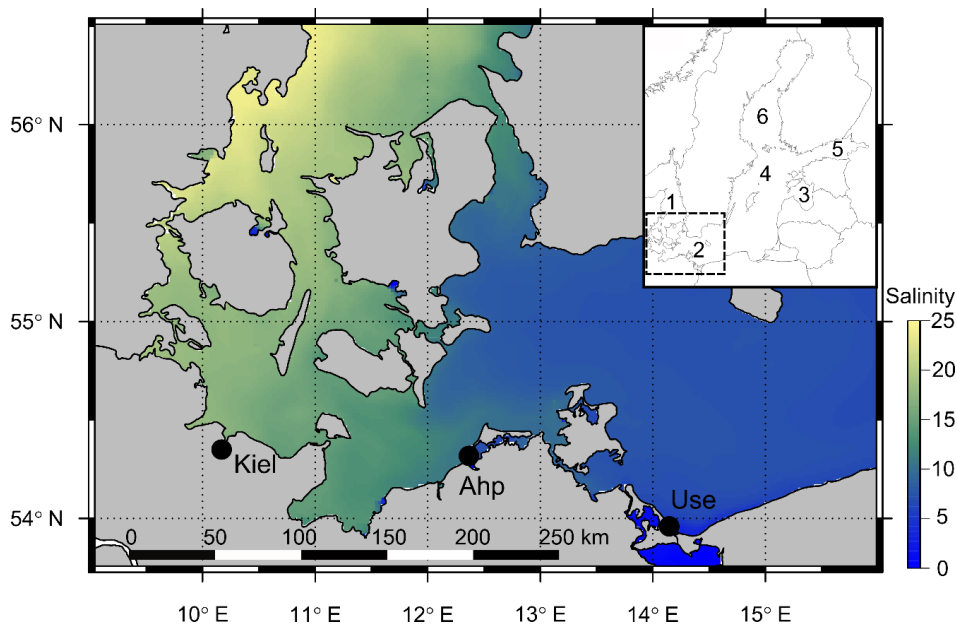


- 775 Wołowicz, M., Sokołowski, A., Bawazir, A. S. and Lasota, R.: Effect of eutrophication on the distribution and ecophysiology of the mussel *Mytilus trossulus* (Bivalvia) in southern Baltic Sea (the Gulf of Gdańsk), *Limnol. Oceanogr.*, 51, 580-590, https://doi.org/10.4319/lo.2006.51.1_part_2.0580, 2006.
- Zeebe, R. E. and Wolf-Gladrow, D. A.: CO₂ in seawater: Equilibrium, kinetics, isotopes, Elsevier Oceanography Series: Amsterdam, 2001.
- 780 Zoccola, D., Ganot, P., Bertucci, A., Caminiti-Segonds, N., Techer, N., Voolstra, C. R., Aranda, M., Tambutté, É., Allemand, D., Casey, J. R. and Tambutté, S.: Bicarbonate transporters in corals point towards a key step in the evolution of cnidarian calcification, *Sci. Rep.*, 5, 9983, <https://doi.org/10.1038/srep09983>, 2015.
- 785
- 790
- 795
- 800
- 805
- 810
- 815
- 820
- 825
- 830



Figures

835 Figure 1: Map of the southwest and Central Baltic Sea depicting the decreasing salinity gradient from the Kattegat (West) to the Baltic Proper (East) with the three field sites shown (Kiel, Ahrenshoop and Usedom). The inset map shows the position of the southwest Baltic Sea (box in inset) in relation to other regions: 1 – Kattegat, 2 – southwest Baltic, 3 – Gulf of Riga, 4 – Central Baltic Proper, 5 – Gulf of Finland and 6 – Bothnian Sea. Salinity data was taken from open source monitoring data (EU, Copernicus Marine Services, 2018; details in supplementary material).



840

845

850

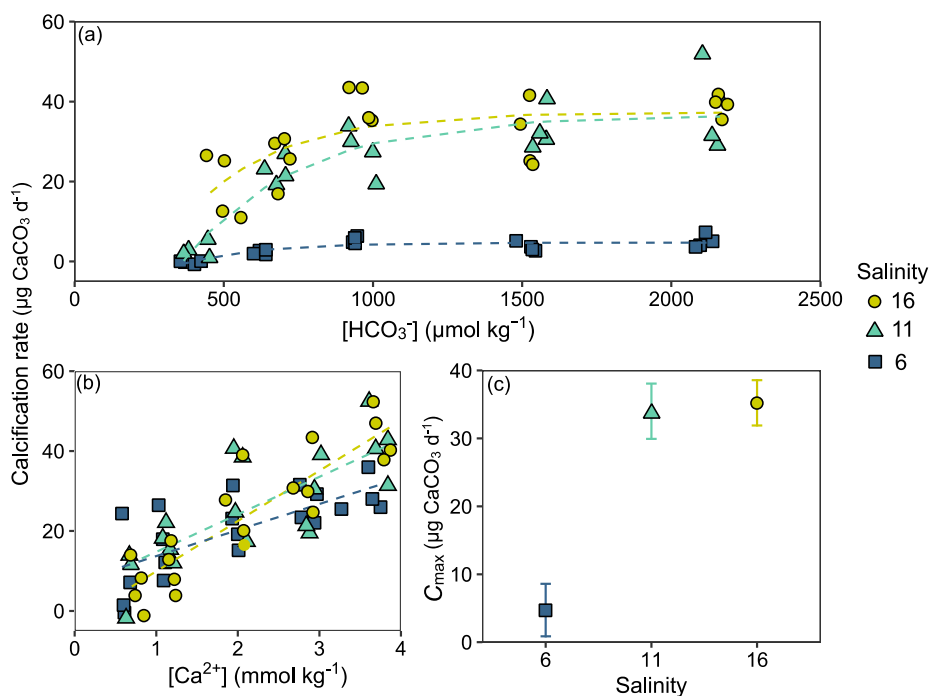
855

860

865



870 Figure 2: Individual calcification rates ($\mu\text{g CaCO}_3 \text{ d}^{-1}$) in both laboratory experiments. Calcification rates across $[\text{HCO}_3^-]$ in the bicarbonate experiment are shown with negative exponential decay models for each salinity treatment (a). Calcification rates across $[\text{Ca}^{2+}]$ in the calcium experiment are fitted with linear trendlines for each salinity treatment (b). The model parameter C_{max} ($\mu\text{g CaCO}_3 \text{ d}^{-1}$) for each salinity in the bicarbonate experiment is depicted $\pm 95\%$ confidence interval (c).



875

880

885

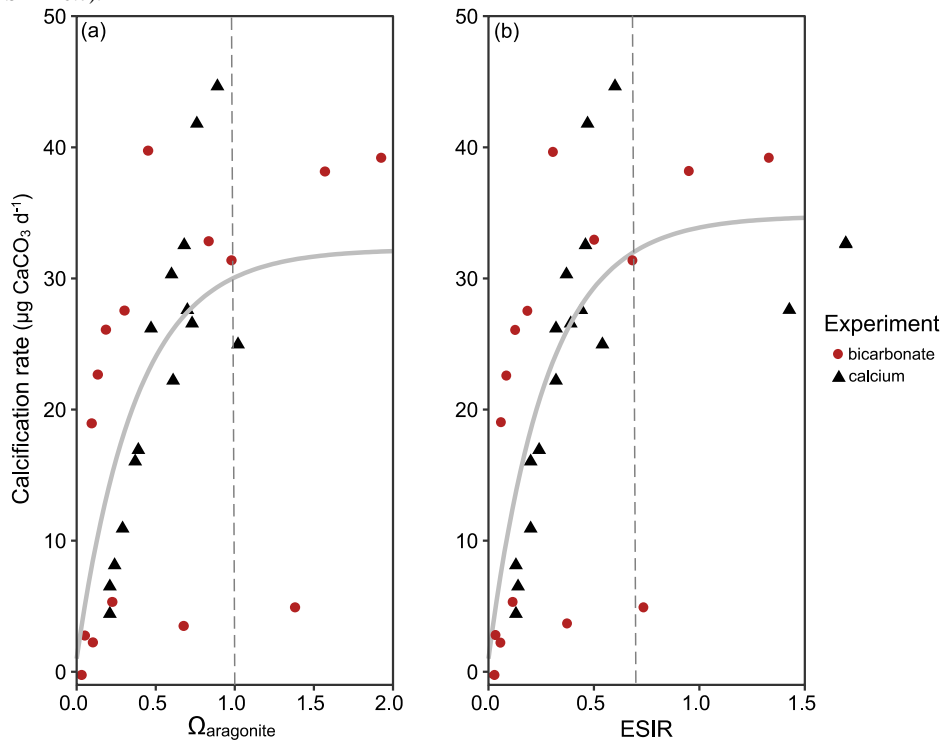
890

895



Figure 3: Calcification rates (means from each treatment) from both laboratory experiments (HCO_3^- , red circles and $[\text{Ca}^{2+}]$, black triangles) across calculated $\Omega_{\text{aragonite}}$ (a) and ESIR ($[\text{Ca}^{2+}][\text{HCO}_3^-] / [\text{H}^+]$) (b). Non-linear negative exponential decay models are graphically presented across both laboratory experiments, and vertical dotted lines represent the theoretical saturation thresholds, below which calcification rates are severely impeded ($\Omega_{\text{aragonite}} = 1$, ESIR = 0.7).

900



905

910

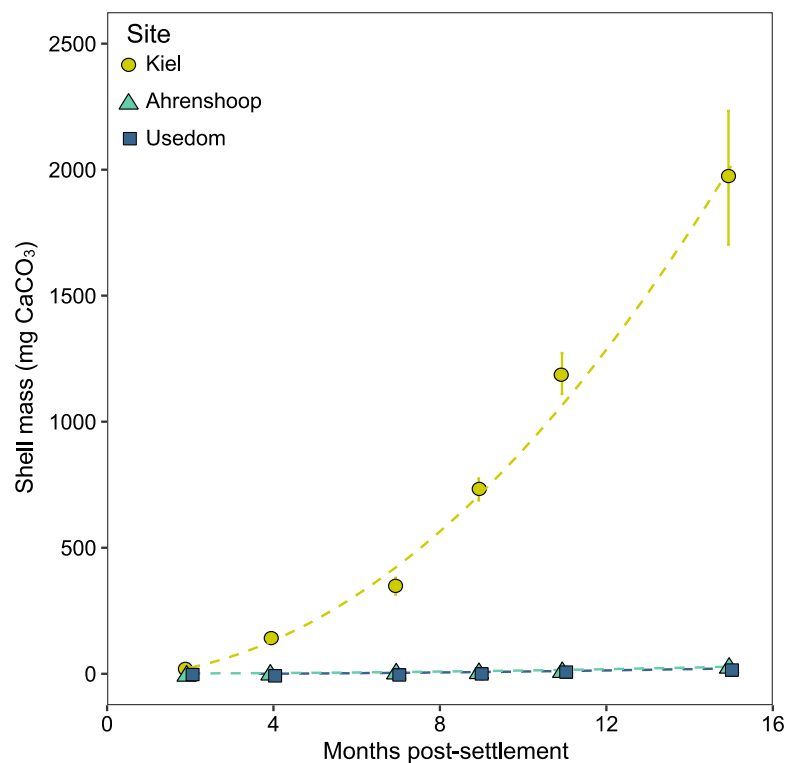
915

920

925



Figure 4: Field calcification over 15 months at the three monitoring sites in the Baltic Sea (Kiel, Ahrenshoop and Usedom). Shell mass was calculated from shell SL-CaCO₃ mass relationships for each population (Fig. S1).



930

935

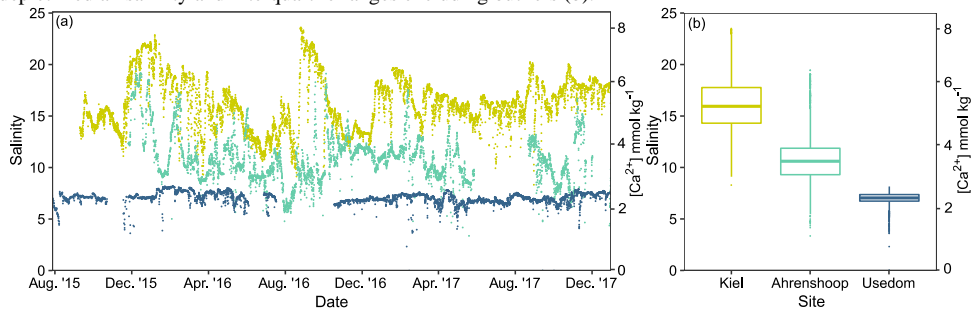
940

945

950



955 Figure 5: Field salinity and $[Ca^{2+}]$ at the three Baltic Sea sites from Aug. 2015-Dec. 2017 (a). Salinity data is derived from deployed CTD loggers and $[Ca^{2+}]$ was calculated from these values (see section 2.5). Box plots depict median salinity and interquartile ranges excluding outliers (b).



960

965

970

975

980

985

990

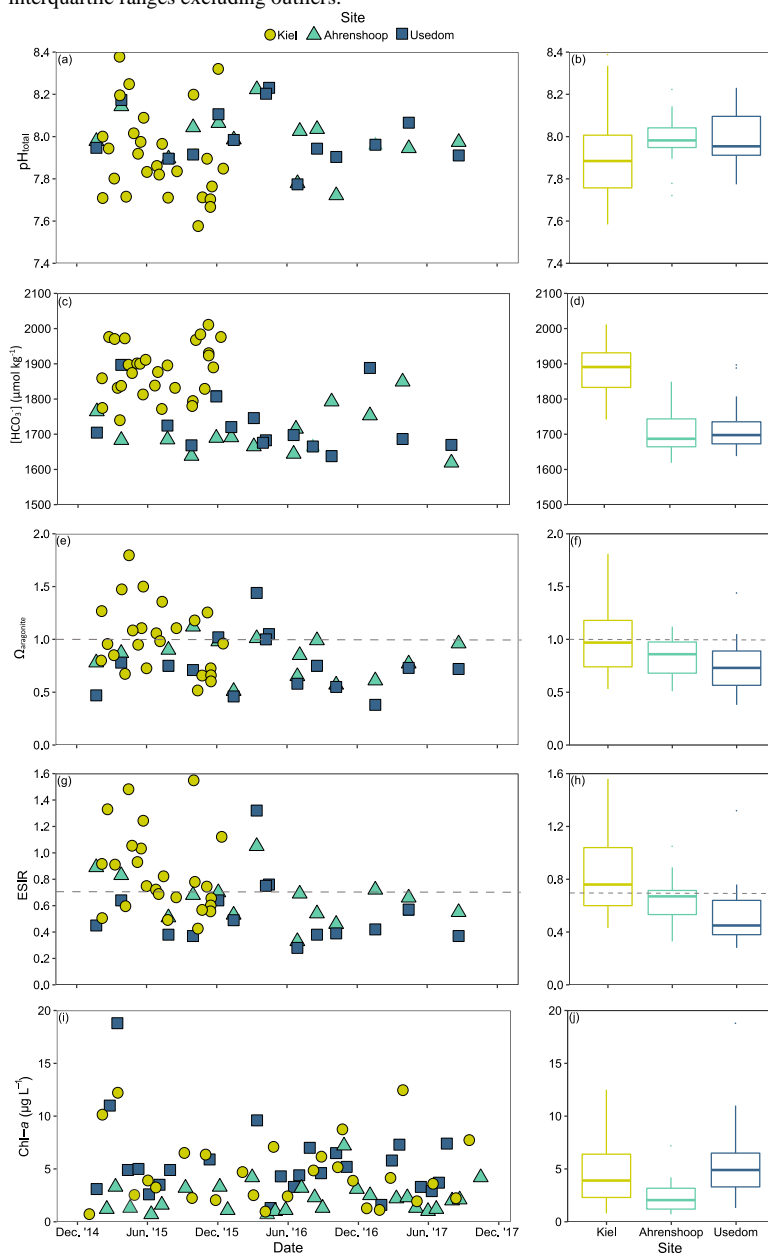
995

1000



1005

Figure 6: Environmental monitoring data from Kiel, Ahrenshoop and Usedom. Values for pH_{total} ($-\log_{10}[\text{H}^+]$) at *in situ* temperatures (a), and associated boxplots (b); $[\text{HCO}_3^-]$ (c), and boxplots (d); $\Omega_{\text{aragonite}}$ with the horizontal dashed line depicting the theoretical saturation threshold of $\Omega_{\text{aragonite}} = 1$ (e), and boxplots (f); extended substrate-inhibitor ratio ($[\text{Ca}^{2+}][\text{HCO}_3^-] / [\text{H}^+]$) with the horizontal dashed line depicting the theoretical saturation threshold of $\text{ESIR} = 0.7$ (g), and boxplots (h); $\text{Chl-}a$ as a proxy for food availability (i), and boxplots (j). Details describing carbonate chemistry calculations are presented in the methods section. Boxplots display median values and interquartile ranges excluding outliers.



1010



1015

Figure 7: A_T -salinity relationship from field monitoring data over the monitoring period for each site showing a linear fit with model parameters given in Table S9. Linear A_T -S relationships (grey dashed lines) for the Gulf of Bothnia, Gulf of Finland and the Kattegat are also depicted, using 2D linear model parameters for 2014 from Müller, et al., 2016. The linear A_T -S relationship for the Gulf of Riga is shown using model parameters for 2008 from Beldowski, et al., 2010.

1020

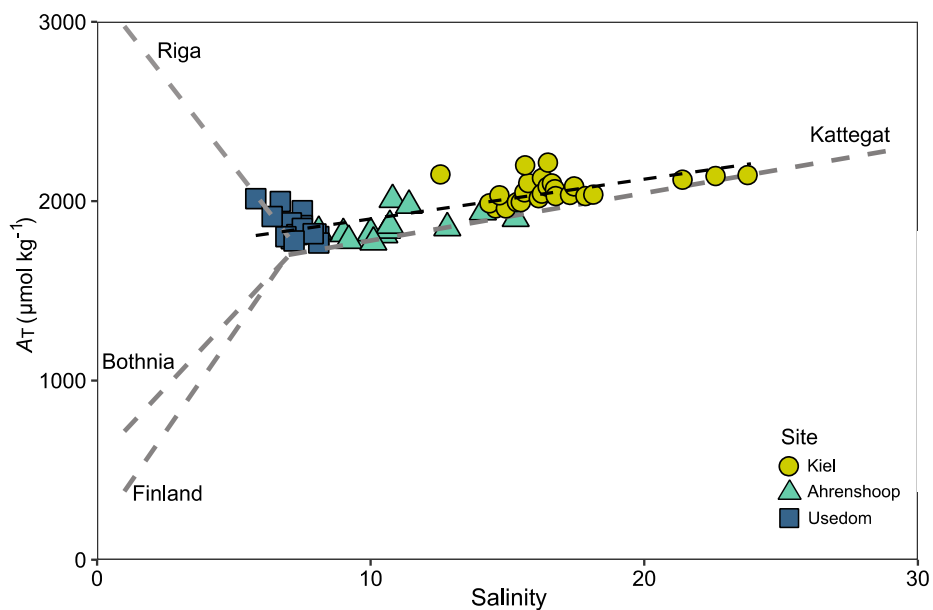




Table 1 Water chemistry parameters for the bicarbonate ion manipulation experiment. Columns from left to right present: Target and Experimental salinity, pH_{total} , partial pressure of carbon dioxide, total alkalinity, total dissolved inorganic carbon, Target and actual bicarbonate ion concentration, carbonate ion concentration, carbon dioxide concentration, calcium ion concentration, aragonite saturation state, substrate inhibitor ratio and extended substrate inhibitor ratio. All carbonate chemistry parameters were calculated using pH_{NBS} and C_{T} as inputs and $[\text{Ca}^{2+}]$ was calculated as described in methods section 2.3. Mean values are presented ($n = 4$) \pm standard deviation (below).

target salinity	salinity	pH_{total}	pCO_2 (μatm)	A_{T} ($\mu\text{mol kg}^{-1}$)	C_{T} ($\mu\text{mol kg}^{-1}$)	target $[\text{HCO}_3^-]$	$[\text{HCO}_3^-]$ ($\mu\text{mol kg}^{-1}$)	$[\text{CO}_3^{2-}]$ ($\mu\text{mol kg}^{-1}$)	CO_2 ($\mu\text{mol kg}^{-1}$)	$[\text{Ca}^{2+}]$ (mmol kg^{-1})	Ω_{arag}	SIR	ESIR
	6.5	7.37	537.4	397.4	417.3		392.4	2.7	22.2	2.5	0.04	0.01	0.02
6.0	± 0.0	± 0.03	± 19.5	± 19.7	± 19.0	300	± 19.0	± 0.3	± 0.8	± 0.0	± 0.01	± 0.00	± 0.00
	6.3	7.57	549.4	643.7	660		630.8	6.5	22.7	2.4	0.11	0.02	0.06
6.0	± 0.0	± 0.01	± 11.3	± 14.1	± 13.7	600	± 13.4	± 0.3	± 0.5	± 0.0	± 0.01	± 0.00	± 0.00
	6.3	7.73	573.7	973.1	982.6		944.7	14.2	23.7	2.4	0.23	0.05	0.12
6.0	± 0.0	± 0.02	± 29.2	± 17.0	± 16.7	900	± 16.1	± 0.7	± 1.2	± 0.0	± 0.01	± 0.00	± 0.01
	6.3	8	493.6	1614.1	1592.4		1529.8	42.2	20.4	2.4	0.69	0.15	0.37
6.0	± 0.0	± 0.01	± 10.5	± 17.0	± 16.0	1500	± 15.1	± 1.2	± 0.4	± 0.0	± 0.02	± 0.00	± 0.01
	6.2	8.17	462.4	2278.6	2214.6		2110.2	85.3	19.1	2.4	1.39	0.31	0.74
6.0	± 0.0	± 0.01	± 5.5	± 22.0	± 20.5	2100	± 19.1	± 1.7	± 0.2	± 0.0	± 0.03	± 0.01	± 0.02
	11.3	7.43	568.2	425.3	443.5		416.9	3.8	22.8	4	0.06	0.01	0.04
11.0	± 0.0	± 0.03	± 26.0	± 22.9	± 22.1	300	± 21.9	± 0.4	± 1.0	± 0.0	± 0.01	± 0.00	± 0.00
	11.2	7.5	648.7	706.7	722.3		687.3	9	26	4	0.14	0.02	0.09
11.0	± 0.0	± 0.03	± 68.3	± 15.8	± 16.0	600	± 15.1	± 0.6	± 2.7	± 0.0	± 0.01	± 0.00	± 0.01
	11.1	7.69	564	1010.5	1011		969.1	19.2	22.6	3.9	0.31	0.05	0.19
11.0	± 0.0	± 0.01	± 14.7	± 26.8	± 25.9	900	± 24.9	± 1.0	± 0.6	± 0.0	± 0.02	± 0.00	± 0.01
	11.1	7.91	539.4	1671.2	1637.1		1563.2	52.2	21.7	3.9	0.84	0.13	0.51
11.0	± 0.0	± 0.01	± 11.4	± 42.9	± 40.3	1500	± 37.8	± 2.6	± 0.5	± 0.0	± 0.04	± 0.01	± 0.03
	11.4	8.06	533.5	2330.2	2252.2		2133	97.8	21.4	3.9	1.58	0.24	0.95
11.0	± 0.0	± 0.01	± 8.5	± 41.5	± 38.1	2100	± 35.1	± 3.4	± 0.3	± 0.0	± 0.06	± 0.01	± 0.03
	16.5	7.35	588.6	522.8	536.7		507.6	6.1	23	5.7	0.1	0.01	0.07
16.0	± 0.0	± 0.02	± 22.5	± 35.6	± 34.9	300	± 33.8	± 0.8	± 0.9	± 0.0	± 0.01	± 0.00	± 0.01
	16.4	7.52	556.8	731.4	736.5		702.9	11.9	21.8	5.7	0.19	0.02	0.13
16.0	± 0.0	± 0.01	± 9.7	± 28.5	± 27.8	600	± 26.7	± 0.8	± 0.4	± 0.0	± 0.01	± 0.00	± 0.01
	16.3	7.7	523.6	1084.8	1070.8		1022.5	27.9	20.5	5.6	0.45	0.06	0.31
16.0	± 0.0	± 0.03	± 4.9	± 70.5	± 66.6	900	± 62.9	± 3.8	± 0.2	± 0.0	± 0.06	± 0.01	± 0.04
	16.3	7.87	547.3	1707	1658.9		1575.6	61.9	21.4	5.6	0.99	0.12	0.69
16.0	± 0.0	± 0.02	± 8.2	± 85.4	± 79.7	1500	± 73.9	± 5.9	± 0.3	± 0.0	± 0.09	± 0.01	± 0.07
	16.2	8.03	555.3	2484.6	2377.7		2235.8	120.2	21.7	5.6	1.93	0.24	1.34
16.0	± 0.0	± 0.01	± 12.5	± 75.4	± 69.7	2100	± 63.8	± 6.5	± 0.5	± 0.0	± 0.10	± 0.01	± 0.07



Table 2 Water chemistry parameters for the calcium ion manipulation experiment. Columns from left to right present: Target and Experimental salinity, pH_{total} , partial pressure of carbon dioxide, total alkalinity, total dissolved inorganic carbon, bicarbonate ion concentration, carbonate ion concentration, carbon dioxide concentration, Target and experimental calcium ion concentration, aragonite saturation state, substrate inhibitor ratio and extended substrate inhibitor ratio. All carbonate chemistry parameters were calculated using pH_{NBS} and C_T as inputs and $[\text{Ca}^{2+}]$ was measured as described in methods section 2.3. Mean values are presented ($n = 4$) \pm standard deviation.

target salinity	salinity	pH_{total}	pCO_2 (μatm)	A_T ($\mu\text{mol kg}^{-1}$)	C_T ($\mu\text{mol kg}^{-1}$)	$[\text{HCO}_3^-]$ ($\mu\text{mol kg}^{-1}$)	$[\text{CO}_3^{2-}]$ ($\mu\text{mol kg}^{-1}$)	CO_2 ($\mu\text{mol kg}^{-1}$)	target $[\text{Ca}^{2+}]$	$[\text{Ca}^{2+}]$ (mmol kg^{-1})	Ω_{arag}	SIR	ESIR
6.0	6	7.99	651.2	1972.5	1927.2	1835.6	64.3	27.9	0.5	0.7	0.24	0.2	0.13
	± 0.1	± 0.12	± 8.3	± 18.4	± 21.5	± 28.2	± 15.0	± 8.3		± 0.0	± 0.06	± 0.05	± 0.03
6.0	6	7.94	716	1961.9	1927.2	1839.9	57.3	30.7	1.0	1.1	0.37	0.18	0.2
	± 0.1	± 0.11	± 8.4	± 20.7	± 21.5	± 24.8	± 12.7	± 8.4		± 0.0	± 0.08	± 0.04	± 0.04
6.0	6.1	7.9	796.9	1954.4	1927.2	1840.2	53.6	34.1	2.0	2	0.61	0.16	0.32
	± 0.1	± 0.12	± 9.0	± 18.4	± 21.5	± 27.3	± 14.7	± 9.0		± 0.0	± 0.17	± 0.04	± 0.09
6.0	6.2	7.85	847.9	1942.4	1927.2	1847.1	44.7	36.2	3.0	2.8	0.73	0.14	0.39
	± 0.2	± 0.08	± 6.5	± 26.3	± 21.5	± 19.5	± 8.3	± 6.5		± 0.0	± 0.13	± 0.03	± 0.07
6.0	6.3	7.88	799.1	1948.4	1927.2	1845.7	48.1	34.1	4.0	3.7	1.02	0.15	0.54
	± 0.1	± 0.09	± 6.3	± 28.0	± 21.5	± 19.4	± 9.7	± 6.3		± 0.1	± 0.21	± 0.03	± 0.11
11.0	10.6	7.95	645.2	1994.5	1936	1839.4	70.3	26.3	0.5	0.7	0.21	0.18	0.13
	± 0.2	± 0.10	± 5.9	± 40.5	± 18.5	± 11.7	± 15.3	± 5.9		± 0.0	± 0.05	± 0.04	± 0.03
11.0	10.6	8.01	565.2	2010.2	1936	1832.1	80.8	23.1	1.0	1.2	0.39	0.2	0.24
	± 0.2	± 0.10	± 4.5	± 43.5	± 18.5	± 17.6	± 22.0	± 4.5		± 0.0	± 0.11	± 0.05	± 0.06
11.0	10.7	7.97	601.7	1999.7	1936	1838.5	73	24.5	2.0	2	0.6	0.18	0.37
	± 0.3	± 0.09	± 4.4	± 38.2	± 18.5	± 13.7	± 15.6	± 4.4		± 0.0	± 0.13	± 0.04	± 0.08
11.0	10.8	7.89	707.7	1978.1	1936	1848.8	58.4	28.8	3.0	3	0.7	0.15	0.44
	± 0.3	± 0.05	± 3.5	± 29.4	± 18.5	± 15.0	± 7.2	± 3.5		± 0.0	± 0.09	± 0.02	± 0.06
11.0	10.8	7.81	839.6	1961.2	1936	1853	48.8	34.2	4.0	3.9	0.76	0.12	0.47
	± 0.3	± 0.04	± 3.0	± 25.0	± 18.5	± 17.0	± 5.7	± 3.0		± 0.1	± 0.09	± 0.01	± 0.05
16.0	15.1	7.95	584.6	2020.3	1940.8	1836.8	80.7	22.8	0.5	0.8	0.2	0.17	0.14
	± 0.2	± 0.07	± 3.2	± 50.5	± 32.2	± 23.5	± 13.2	± 3.2		± 0.0	± 0.0	± 0.03	± 0.02
16.0	15.1	7.94	599.1	2015.2	1940.8	1839.9	77	23.3	1.0	1.2	0.3	0.16	0.2
	± 0.2	± 0.05	± 2.6	± 46.4	± 32.2	± 25.2	± 9.6	± 2.6		± 0.0	± 0.0	± 0.02	± 0.03
16.0	15.3	7.92	614.1	2011.5	1940.8	1842	74.3	23.8	2.0	2	0.5	0.16	0.32
	± 0.2	± 0.04	± 1.9	± 43.3	± 32.2	± 26.5	± 7.7	± 1.9		± 0.0	± 0.0	± 0.02	± 0.03
16.0	15.4	7.9	646.8	2007.1	1940.8	1843.3	71.8	25.1	3.0	3	0.7	0.15	0.46
	± 0.2	± 0.05	± 2.6	± 45.4	± 32.2	± 25.9	± 9.1	± 2.6		± 0.1	± 0.1	± 0.02	± 0.06
16.0	15.4	7.91	647.5	2010.7	1940.8	1840.2	74.8	25.2	4.0	3.8	0.9	0.16	0.6
	± 0.2	± 0.07	± 3.9	± 52.0	± 32.2	± 23.6	± 13.4	± 3.9		± 0.0	± 0.2	± 0.03	± 0.11



Table 3. Summary of environmental conditions and field calcification rates for the experimental monitoring period (2015-2018) at the three Baltic Sea localities (Kiel, Ahrenshoop, Usedom). Salinity and temperature were recorded using mini-CTD's, pH_{total} , C_T and A_T were measured in laboratory conditions with pCO_2 , $[\text{HCO}_3^-]$ and $\Omega_{\text{aragonite}}$ calculated on CO2Sys_v2.1 programme using pH_{total} and C_T as inputs. $[\text{Ca}^{2+}]$ and the ESIR were calculated from carbonate, salinity and carbonate chemistry parameters respectively. The chl-*a* data presented originates from physical monitoring data (see methods section 2.8). Calcification rates represent the linear slope coefficients of calcification over time (days) at each site with linear model parameters given in Table S10. Mean values are presented \pm standard deviation (below).

site	salinity	temp. (°C)	Chl- <i>a</i> (mg L ⁻¹)	pH_{total}	$[\text{Ca}^{2+}]$ (mmol kg ⁻¹)	pCO_2 (μatm)	$[\text{HCO}_3^-]$ ($\mu\text{mol kg}^{-1}$)	A_T ($\mu\text{mol kg}^{-1}$)	Ω_{arag}	ESIR	calc. rate ($\mu\text{g CaCO}_3 \text{d}^{-1}$)
Kiel	15.2 \pm 3.1	11.2 \pm 5.1	4.68 \pm 3.23	7.94 \pm 0.22	4.99 \pm 0.91	624 \pm 292	1883 \pm 74	2071 \pm 67	1.17 \pm 0.51	1.05 \pm 0.60	2202.9 \pm 37.64
Ahp	10.9 \pm 2.3	10.3 \pm 5.8	2.25 \pm 1.45	7.98 \pm 0.13	3.87 \pm 0.75	506 \pm 172	1704 \pm 65	1858 \pm 72	0.83 \pm 0.19	0.65 \pm 0.19	36.4 \pm 53.2
Use	7.0 \pm 0.6	10.2 \pm 6.4	5.52 \pm 3.59	8.03 \pm 0.18	2.63 \pm 0.17	508 \pm 186	1725 \pm 79	1856 \pm 79	0.76 \pm 0.28	0.55 \pm 0.26	18.6 \pm 53.2